

AWARD NUMBER: W81XWH-15-C-0148

TITLE: BURN INJURY ASSESSMENT TOOL WITH MORPHABLE 3D HUMAN BODY MODELS

PRINCIPAL INVESTIGATOR:

Kay Sun

CONTRACTING ORGANIZATION:

CFD RESEARCH CORPORATION
701 McMillian Way NW, Suite D
HUNTSVILLE, AL 35806-2923

REPORT DATE:

4/22/2016

TYPE OF REPORT: Final

PREPARED FOR: U.S. Army Medical Research and Materiel Command
Fort Detrick, Maryland 21702-5012

DISTRIBUTION STATEMENT: Approved for Public Release;
Distribution Unlimited (**SBIR Data Rights**)

The views, opinions and/or findings contained in this report are those of the author(s) and should not be construed as an official Department of the Army position, policy or decision unless so designated by other documentation.

REPORT DOCUMENTATION PAGE

*Form Approved
OMB No. 0704-0188*

Public reporting burden for this collection of information is estimated to average 1 hour per response, including the time for reviewing instructions, searching existing data sources, gathering and maintaining the data needed, and completing and reviewing this collection of information. Send comments regarding this burden estimate or any other aspect of this collection of information, including suggestions for reducing this burden to Department of Defense, Washington Headquarters Services, Directorate for Information Operations and Reports (0704-0188), 1215 Jefferson Davis Highway, Suite 1204, Arlington, VA 22202-4302. Respondents should be aware that notwithstanding any other provision of law, no person shall be subject to any penalty for failing to comply with a collection of information if it does not display a currently valid OMB control number. PLEASE DO NOT RETURN YOUR FORM TO THE ABOVE ADDRESS.

1. REPORT DATE 4/22/2016			2. REPORT TYPE SBIR Final Report			3. DATES COVERED 9/24/15 - 4/22/2016		
4. TITLE AND SUBTITLE BURN INJURY ASSESSMENT TOOL WITH MORPHABLE 3D HUMAN BODY			5a. CONTRACT NUMBER W81XWH-15-C-0148					
			5b. GRANT NUMBER					
			5c. PROGRAM ELEMENT NUMBER					
6. AUTHOR(S) Kay Sun, Michael Rossi, Xianlian (Alex) Zhou, Andrzej Przekwas, Vincent Harrand, Keith Sedberry – CFD Research Corporation David Herndon – University of Texas Medical Branch			5d. PROJECT NUMBER					
			5e. TASK NUMBER					
			5f. WORK UNIT NUMBER					
7. PERFORMING ORGANIZATION NAME(S) AND ADDRESS(ES) CFD RESEARCH CORPORATION 701 McMillian Way NW, Suite D HUNTSVILLE, AL 35806-2923			8. PERFORMING ORGANIZATION REPORT NUMBER 9199/Final					
9. SPONSORING / MONITORING AGENCY NAME(S) AND ADDRESS(ES) U.S. Army Medical Research and Materiel Command Fort Detrick, Maryland 21702-5012			10. SPONSOR/MONITOR'S ACRONYM(S)					
			11. SPONSOR/MONITOR'S REPORT NUMBER(S)					
12. DISTRIBUTION / AVAILABILITY STATEMENT Approved for Public Release; Distribution Unlimited								
13. SUPPLEMENTARY NOTES								
14. ABSTRACT Burn patient outcomes are dependent on the wound surface area as a percent of the total body surface area (%TBSA), burn locations, burn depth, and patient age. %TBSA is essential in determining fluid resuscitation and nutrition support, and surgical intervention and rehabilitation planning. The proposed burn injury assessment software tool is aimed at increasing %TBSA accuracy by improving on both TBSA and burn area estimations. Conventional methods (Rule-of-Palm/Nines and Lund-Browder chart) use a generic 2D body shape diagram to represent the human body which lacks the capability to capture 3D anthropometric variability of actual human body shapes, resulting in inaccurate %TBSA. This burn assessment tool will include an interactive anthropometry-based human body generator to create, in real-time, a personalized 3D body shape model that has been morphed according to available subset of adjustable anthropometric measurements (weight, age, gender, height, waist, arms and legs measurements) as stored in most anthropometry databases. To improve on burn area estimations, the burn tool will allow the user to interactively demarcate burn areas of varying severity directly on the personalized 3D model for calculation of %TBSA. Further enhancements will involve the use of available photographic images of burned body parts to assist in burn demarcation.								
15. SUBJECT TERMS Burns, Burn size, Burn assessment, Over-resuscitation, 3D anthropometry modeling, Anthropometric morphing, Cutaneous functional units, Image assisted burn assessment, Computer aided burn assessment.								
16. SECURITY CLASSIFICATION OF:			17. LIMITATION OF ABSTRACT Unclassified	18. NUMBER OF PAGES 60	19a. NAME OF RESPONSIBLE PERSON Kay Sun			
a. REPORT Unclassified	b. ABSTRACT Unclassified	c. THIS PAGE Unclassified			19b. TELEPHONE NUMBER (include area code) 256-726-4800			

TABLE OF CONTENTS

1.	INTRODUCTION	1
1.1.	Project Scope.....	1
1.2.	Project Purpose and Significance.....	1
2.	OVERALL PROJECT SUMMARY	2
2.1.	Task 1: Software Requirements Analysis and Design	2
2.1.1.	Project Initiation	2
2.1.2.	Burn Management and Workflow	2
2.2.	Task 2: Anthropometric Body Shape Generation	6
2.2.1.	3D Principal Component Analysis (PCA) of ANSUR II Body Scans	6
2.2.2.	Anthropometry Body Features and Landmarks.....	7
2.2.3.	Relation Between 3D PCA and Traditional Measurement.....	16
2.2.4.	Feature Comparisons between 3D PCA Models and Measurements	16
2.3.	Task 3: Cutaneous Functional Unit Classification of the Anthropometry Models	20
2.4.	Task 4: Develop Model Surface Demarcation Tools	23
2.5.	Task 5: Calculation and Validation of Burn Surface Area.....	25
2.6.	Task 6: GUI Design and Development	27
2.6.1.	Anthropometric Body Generation	27
2.6.2.	CFU	32
2.6.3.	Demarcation Tools	35
2.6.4.	Burn Area Reporting	37
2.6.5.	Image Assist Demarcation.....	38
2.7.	Task 7: Project Management, Planning and Commercialization	41
3.	KEY RESEARCH ACCOMPLISHMENTS	42
4.	CONCLUSION.....	43
4.1.	Project Importance and Implications.....	43
4.2.	Work Plans for Phase II	43
5.	PUBLICATIONS, ABSTRACTS, AND PRESENTATIONS	46
6.	INVENTIONS, PATENTS AND LICENSES	47
7.	REPORTABLE OUTCOMES.....	47
8.	OTHER ACHIEVEMENTS	49
9.	REFERENCES	50
10.	APPENDICES	52

LIST OF FIGURES

Figure 1: Demarcation of burn areas on morphed 3D human body models.....	1
Figure 2: (a) Key questions to ascertain burn history [3] and (b) additional tests required for different causes of burns and injuries [3].....	2
Figure 3: (a) Initial assessment of burn injury [3] and (b) flow chart for primary survey of a burn injury [3].	3
Figure 4: Signs and indications for airway management [3].....	3
Figure 5: (a) Rule-of-Nines and (b) Lund and Browder chart [5].	5
Figure 6: List of past and current fluid resuscitation formulas [11].	6
Figure 7: Examples of impractical and insignificant ANSUR II anthropometry measurements eliminated from the body feature list [13] include (a) forearm-forearm breath, (b) vertical trunk circumference, (c) interscye ii, and (d) crotch length.....	8
Figure 8: Illustration of problematic body features that includes (a) head_circum and (b) waist_front_length.	10
Figure 9: (a) Smoothed back of head to correct for the hair bun in the mean female body surface mesh, (b) protrusion and (c) smoothing areas (highlighted in red) at the back of the head in a generated body surface case.....	10
Figure 10: Front and back view of the all the landmarks (blue spheres) on the (a) male and (b) female body.....	11
Figure 11: Body feature measurements (red lines).....	16
Figure 12. Comparison between 3D features and their corresponding traditional measurements for (a) male and (b) female.	19
Figure 13. Measurement of chest_breadth as defined in (a) ANSUR II and (b) computed in our Anthropometry software tool.....	20
Figure 14. CFDRC's CFU classification based on the schema developed by Richard et al. [2] on the mean male body. (a) Front view of the colored CFUs on the mean male 3D body, and (b) and (c) are the corresponding CFDRC's CFU definitions in the front. (d) Back view of the colored CFUs on the mean male 3D body, and (e) and (f) are the corresponding CFDRC's CFU definitions in the back. (g) Colored CFU classification of the mean male head corresponds to (h) CFDRC's CFU definitions.....	21
Figure 15. The CFU classification follows the morphing of the male body shapes.....	22
Figure 16. The same CFU classification schema was applied to the mean female body with the (a) front, (b) and (c) side views. This classification also follows the morphing of the female body shapes shown in (d), (e) and (f).	23
Figure 17. Mesh surface demarcation tool with (a) addition using a larger sized circle brush and (b) erasing with a smaller sized circle brush. Different burn severity (full (red), deep (orange), partial (yellow) and superficial (green)) and amputation (black) demarcations are color coded.....	24
Figure 18. Different demarcated burn severity (full burn (red), deep burn (orange), partial burn (yellow) and superficial burn (green)) surfaces morphs with the full body surface in real-time.	24
Figure 19: Average absolute errors between TBSAs calculated using our software tool and the formula based BSAs for the 1000 randomly generated (a) male and (b) female bodies. The error bars denote 1 standard deviation from the mean.....	26

Figure 20: %TBSA for head/neck, torso, arms, legs, and groin calculated using our software tool and Rule-of-Nines method for the 1000 randomly generated (a) male and (b) female bodies. The error bars denote the range of the %TBSA values.	27
Figure 21. Screenshot of the software tool upon initialization with the male model automatically loaded and the biographical information and default anthropometry features (height, weight and waist circumference) displayed for the user to input.	28
Figure 22. Screenshot of the tool with female gender selected and advance anthropometry features selected for the user to input.	29
Figure 23. Examples of arbitrary (a) male and (b) anthropometric models.....	30
Figure 24. In the Landmarks tab, the display of body landmarks are controlled and visualized as blue spheres. Positional information of that point is displayed on the right panel and can be adjusted if necessary.	30
Figure 25: (a) The model automatically becomes semi-transparent when visualizing anthropometry features. (b) Hiding the features restores the full opacity of the model.	31
Figure 26. (a) CFU tab in the GUI where CFU codes are grouped based on hierarchy in the CFU tab of the GUI. All 144 CFU codes are listed in descending order from b to e.....	33
Figure 27. Visibility of each CFU can be controlled individually or in selected groups.	34
Figure 28: Examples of the improved keyword search of the CFUs. (a) Searching with main body segment keywords, such as right leg, and (b) lower hierarchical keywords, such as cheek, will result in the entire CFU displayed.....	34
Figure 29. Screenshot of the GUI with the 4 different burn severity selections highlighted in different colors (full (red), deep (orange), partial (yellow) and superficial (green)) along with black for amputation. (a) When paint brush icon is pressed, an adjustable slider controlling the size of the circular painting brush appears (boxed in red). (b) Interactive erasing of highlighted demarcations. A clear selection icon is available for deleting all selections for specific demarcation (boxed in blue). (c) Visibility of all demarcations can be controlled by toggling the respective push buttons. In this example, demarcations for full burn are hidden, while the rest are made visible.....	36
Figure 30. Screenshot of the TBSA tab in the burn assessment tool upon initialization.....	37
Figure 31. Screenshots of the TBSA report in (a) percentage and (b) absolute cm ² . At the bottom, total burn areas for each burn severity plus amputation are listed on the top along with just the CFUs that are demarcated. Both are color coded based on burn severity. At the top is the fluid recommendation according to Brooke and Parkland formulae.	38
Figure 32. Screenshots of the image assisted demarcation. (a) The initial superpositioning of the loaded image (boxed in red) on top of the 3D model and the automatic appearance of the transparency control slider (boxed in blue). (b) Adjustment of the transparency slider changes the opacity of the loaded image for better visualization during manual alignment and tracing. (c) Tracing of the burn areas with different severity based on the image onto the 3D model and calculation of burn areas as percentage as well as fluid recommendations. (d) Calculated burn surface areas in cm ² and fluid recommendations with image overlay turned off. The burn image shown was download from http://burnssurgery.blogspot.com [28].	41
Figure 33. Our burn injury assessment software prototype, CoBi_Burn.....	48
Figure 34. Cover slide to the project update and software demonstration meeting with USAIRS.	48

LIST OF TABLES

Table 1. List of male and female body features selected for their feasibility and practicality to acquire and their measurement type. Male only feature is highlighted.....	8
Table 2. Description of the all body landmark locations [13]	11
Table 3. Comparison between 3D features and their corresponding traditional measurements for male and female. Units are in meters unless otherwise indicated.....	17
Table 4: Human body surface area formulas.	25

1. INTRODUCTION

1.1. Project Scope

The overall objective of this project is to develop a burn injury assessment tool with morphable 3D anthropometric human body models in order to improve the accuracy of percentage burn surface area estimates. The goal of Phase I is to develop a functional prototype tool for real-time generation of an anthropometric 3D virtual human body with graphical annotations of burn areas and severity as well as assessment of percentage of total body surface area (%TBSA). The main tasks of this Phase I project are:

1. Generate in real-time virtual 3D human body model representation of the burn patient.
2. Classify the morphable human body template into cutaneous functional units (CFU).
3. Develop user tools for the visual annotation of burn areas and severity as well as calculations of burn areas.
4. Explore the use of photographic images of burned body parts to assist in burn demarcations.

This DoD Army SBIR Phase I project started on 09/24/2015 and was completed on 04/23/2016. This project is conducted by the Computational Medicine and Biology (CMB) Division of CFD Research Corporation (CFDRC) in Huntsville, AL. in collaboration with Professor David N. Herndon of the University of Texas Medical Branch at Galveston (UTMB) who served in this project as the Scientific Consultant.

1.2. Project Purpose and Significance

Burn patient outcomes are dependent on the surface area of the wound as %TBSA, burn location(s) on the body, depth of the burn(s), and age of the patient. %TBSA is essential in determining burn casualty treatment [1] and rehabilitation [2]. Conventional methods (Rule-of-Palm/Nines and Lund-Browder chart) may result in inaccurate %TBSA since they use a generic 2D body shape diagram to represent the human body. This fixed 2D template lacks the capability to capture 3D anthropometric variability of actual human body shapes. The objective of this project is to develop a burn injury assessment software tool that can create anthropometrically realistic 3D virtual human body models in real-time using anthropometry inputs. This 3D human body model will be used to demarcate burn areas based on burn severity and compute %TBSA. Figure 1 illustrates examples of the demarcated burn areas on morphed 3D human body models.

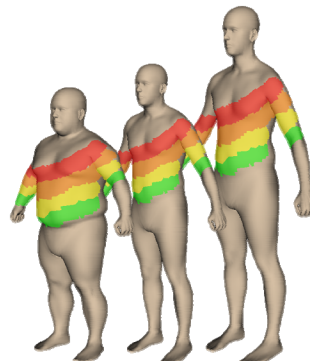


Figure 1: Demarcation of burn areas on morphed 3D human body models.

2. OVERALL PROJECT SUMMARY

The following sections describe work performed and results obtained for each task in the project.

2.1. Task 1: Software Requirements Analysis and Design

2.1.1. Project Initiation

Discussions with our consultant, Prof. Herndon, on the practicality of taking anthropometry body measurements were carried out and the list of measurements for use in body shape morphing were narrowed down (Section 2.2.2). Not all body measurements are required, redundancies have been included in case some measurements cannot be taken due to location of burn or other injuries and mobility of patient. Length and limb circumferences are ideally easier to acquire than hip, waist and chest circumferences especially if the patient is lying down. In that scenario, waist and chest widths and depths may be more straightforward to measure. The more body measurement inputs provided, the more accurate the generated virtual body will be. It will take a few minutes to measure the patient's body features and enter them into the software tool before assessment of burn injury extent can begin. This list of body features can be expanded or even further reduced if desired and will evolve with sensitivity testing during testing and validation. A kickoff meeting with the project team from U.S. Army Institute of Surgical Research (USAISR) to detail the practical expectations of the software was held on October 26th 2015.

2.1.2. Burn Management and Workflow

Upon arrival at the hospital, a thorough patient history is acquired first, preferable first hand, which can provide critical information about the cause, duration and extent of the burn, burn depth, possibility of inhalation and/or other injuries, and patient's pre-existing medical problems. Figure 2a lists a sampling of burn history questions. Further verbal communications at a later time may be hindered by intubation administered due to possible airway swelling hours after burn injury. Based on the cause of burns and injuries, e.g. electrical, inhalation, etc., additional tests such as cardiac enzymes, blood gas analysis, and others will be required (Figure 2b).

Key points of a burn history	
Exact mechanism	<ul style="list-style-type: none">● Type of burn agent (scald, flame, electrical, chemical)● How did it come into contact with patient?● What first aid was performed?● What treatment has been started?
Exact timings	<ul style="list-style-type: none">● When did the injury occur?● How long was patient exposed to energy source?● How long was cooling applied?● When was fluid resuscitation started?
Exact injury	<ul style="list-style-type: none">● What was the liquid? Was it boiling or recently boiled?● If tea or coffee, was milk in it?● Was a solute in the liquid? (Raises boiling temperature and causes worse injury, such as boiling rice)
<i>Scalds</i>	<ul style="list-style-type: none">● What was the voltage (domestic or industrial)?● Was there a flash or arcing?● Contact time
<i>Electrocution injuries</i>	<ul style="list-style-type: none">● What was the chemical?
<i>Chemical injuries</i>	

(a)

Investigations for major burns*	
General	<ul style="list-style-type: none">● Full blood count, packed cell volume, urea and electrolyte concentration, clotting screen● Blood group, and save or crossmatch serum
Electrical injuries	<ul style="list-style-type: none">● 12 lead electrocardiography● Cardiac enzymes (for high tension injuries)
Inhalational injuries	<ul style="list-style-type: none">● Chest x ray● Arterial blood gas analysis <p>Can be useful in any burn, as the base excess is predictive of the amount of fluid resuscitation required Helpful for determining success of fluid resuscitation and essential with inhalational injuries or exposure to carbon monoxide</p>
<small>*Any concomitant trauma will have its own investigations</small>	

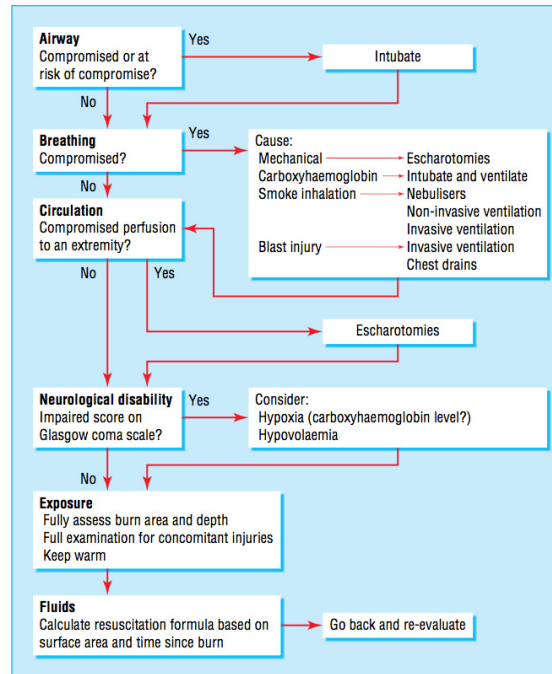
(b)

Figure 2: (a) Key questions to ascertain burn history [3] and (b) additional tests required for different causes of burns and injuries [3].

Burn patients are trauma patients and require rapid injury assessment in accordance with the Advanced Trauma Life Support (ATLS) protocol. Figure 3a lists the steps involved in assessing a burn patient, which includes performing an ABCDEF primary survey, determining the need for analgesia and possible transfer to a specialized burn facility. The ABCEDF primary survey for burn injury is summaries in the flow chart in Figure 3b and it involves:

Initial assessment of a major burn

- Perform an ABCDEF primary survey
 - A—Airway with cervical spine control, B—Breathing, C—Circulation, D—Neurological disability, E—Exposure with environmental control, F—Fluid resuscitation
- Assess burn size and depth
- Establish good intravenous access and give fluids
- Give analgesia
- Catheterise patient or establish fluid balance monitoring
- Take baseline blood samples for investigation
- Dress wound
- Perform secondary survey, reassess, and exclude or treat associated injuries
- Arrange safe transfer to specialist burns facility



(a)

(b)

Figure 3: (a) Initial assessment of burn injury [3] and (b) flow chart for primary survey of a burn injury [3].

A – Airway with cervical spine control

Assess whether airway is compromised or at-risk of compromise. Inhalation of hot gases may cause swelling of airways after a few hours and will require repeated reassessments. Figure 4 lists signs of inhalation injury and indications for intubation.

Airway management

Signs of inhalational injury

- History of flame burns or burns in an enclosed space
- Full thickness or deep dermal burns to face, neck, or upper torso
- Singed nasal hair
- Carbonaceous sputum or carbon particles in oropharynx

Indications for intubation

- Erythema or swelling of oropharynx on direct visualisation
- Change in voice, with hoarseness or harsh cough
- Stridor, tachypnoea, or dyspnoea

Figure 4: Signs and indications for airway management [3].

B – Breathing

All burn patients need to receive 100% oxygen through humidified non-rebreathing mask. This treatment is particularly useful for carbon monoxide poisoning. Pulse oximetry is not able to differentiate between haemoglobin bound to oxygen and to carbon monoxide, only blood gas analysis will reveal elevated carboxyhaemoglobin levels. For deep or full thickness circumferential burns of the chest, the reduced burned tissue elasticity can restrict thoracic excursion during breathing, limiting proper ventilation and requiring escharotomies. In the case of explosions, penetrating injuries to the lungs can result in respiratory distress due to tension pneumothoraces, lung contusions and alveolar trauma. Ashes and products of combustion are irritants to the lungs and can also obstruct normal respiration, resulting in bronchospasm, inflammation, and bronchorrhea [3].

C – Circulation

Two peripheral intravenous accesses are typically sufficient for patients with less than 30% burns. For patients with more significant burns or inhalation injury, a central line placement may be required [4]. Blood can also be taken via these access points to check for blood count, urea and electrolytes, blood group, and clotting screen. Peripheral circulation must be assessed as any deep or full thickness burns to extremities can result in edema after fluid resuscitation. Escharotomies may also be necessary to alleviate tissue pressure from reduced tissue elasticity and facilitate circulation [3].

D – Neurological disability

All burn patients need to be assessed with the Glasgow Coma Scale to ascertain the conscious state and responsiveness of the patient [3].

E – Exposure with environmental control

Perform a complete and thorough physical examination of the entire body of the burn patient to assess the extent of burns and to check for any concomitant injuries. Also, ensure burn patients are kept warm as they are more susceptible to hypothermia, especially in children [3].

F – Fluids

Major burns may trigger increased permeability of capillaries, forcing fluid to leave the blood vessels and accumulate in the burned tissue, resulting in edema. The loss of fluid can exacerbate to hypovolemia and lead to shock and shock-related renal failure. The fluid lost must be replaced to maintain function to all organs and tissue perfusion to burn area. The amount and timing of the administration of fluid is particularly crucial. The movement of fluid from intravascular to interstitial fluid compartments generally occurs during the first 8 to 24 hours, and the exact amount of fluids must be introduced during this time. Insufficient fluid will cause hypoperfusion, while too much fluid will lead to edema and cause tissue hypoxia [5]. Forty-eight to 72 hours and beyond, the swelling will abate as excess fluid in the burn area returns to the blood stream.

Burn Areas

Fluid resuscitation regimens are determined based on estimated burns areas. Great care must be taken not to include erythema and to remove all loose epidermal layers especially for pigmented skin [5]. There are 3 traditional ways to determine %TBSA, Rule-of-Palm [6], Rule-of-Nines [7], and Lund-Browder chart [8]. The Rule-of-Palm uses the patient's hands as a rough reference,

representing about 1% of the TBSA, to visually estimate the %TBSA. However, Rossiter et al. [6] showed that the average palm surface area is actually only 0.76% to 0.78% of the TBSA, indicating an overestimation of 10 to 20% with this method. Both the Rule-of-Nines and Lund-Browder chart use standard 2D generic body diagrams to represent body shape (Figure 5). The Rule-of-Nines divides the generic body diagram into segments, each representing about 9% of the TBSA [9]. %TBSA is thereby determined by estimating the burn areas in each segment and summing the percentages up. To improve the accuracy from the Rule-of Nines method, the Lund-Browder chart further divides the generic body diagram into more regions of varying %TBSA with adjustments for children according to age. It is the most commonly used %TBSA estimation method due to its simplicity, practicality [8] and applicability to children. Since generic body diagrams and fixed %TBSA for each body segment are used, both the Rule-of-Nines and Lunder-Browder chart may overestimate the %TBSA for any individual with high Body Mass Index (BMI) and underestimate for those with low BMI [10] due to their inadaptability to body shape and weight. Human body shapes show enormous variability due to age, gender (women's breasts), physical deformities (e.g. amputation) and physical states, such as height, waist and hip circumference, arms and legs lengths, etc. All these factors can alter an individual's TBSA and burn area, hence %TBSA and ultimately the amount of fluid administered. One of the aims of this burn assessment tool is to therefore account for the human body shape variations by developing an interactive anthropometry-based human body generator to create, in real-time, a personalized 3D body shape model that has been morphed according to available anthropometric measurements (weight, age, gender, height, waist, arms and legs measurements).

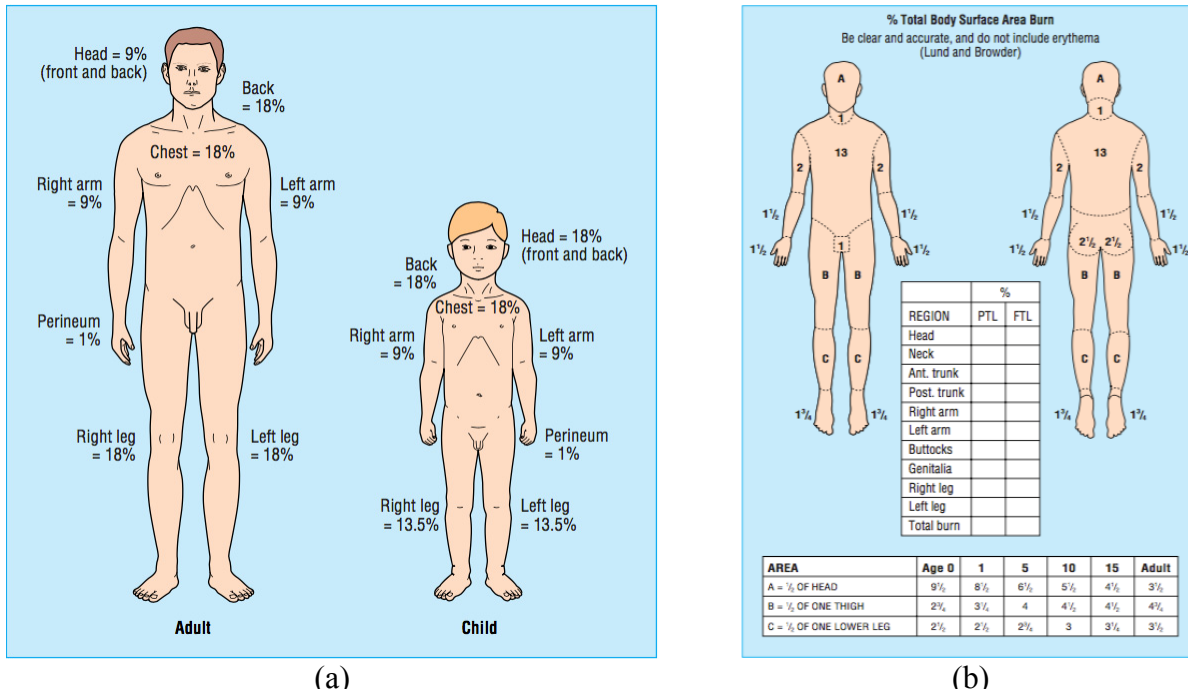


Figure 5: (a) Rule-of-Nines and (b) Lund and Browder chart [5].

Resuscitation Regimens

Fluid resuscitation is typically recommended for %TBSA greater than 15% in adults and more

than 10% in children. There are a number of different fluid resuscitation regimens and all are only guidelines (Figure 6). Fluids administered should not just be based on %TBSA alone but must be continuously adjusted using urine output and other physiological parameters such as blood pressure, respiratory rate, pulse, etc. The ideal urine output to strive for is 0.5 to 1.0 mL/kg/hour for adults, and 1.0 to 1.5 mL/kg/hour in children [5]. Furthermore, patients with large burns require intravenous morphine at doses proportional to body weight and the need for further analgesia reassessed every 30 minutes [3].

-
- Crystalloid formulas: Usually use lactated Ringer's solution, although newer isotonic fluids may be used.
- Parkland (Baxter) formula: 4 ml/kg/% TBSA burn, give half in the first 8 hours and half in the next 16 hours. Adjust rate based on urine output. For second 24 hours, give 20% to 60% of calculated plasma volume as colloid. (The recommendation for the second 24 hours is usually not followed.)
- Modified Brooke formula: 2 ml/kg/% TBSA burn, give half in the first 8 hours and half in the next 16 hours. Adjust rate based on urine output. For the second 24 hours, give 0.33 to 0.5 ml/kg/% TBSA burn as colloid plus D₅W to maintain urine output.
- Hypertonic formulas: No colloid.
- Monaflo: 250 mEq/liter Na⁺ + 150 mEq lactate + 100 mEq Cl⁻. Adjust rate based on urine output. For second 24 hours, give one third of isotonic salt orally.
- Warden: lactated Ringer's plus 50 mEq NaHCO₃ (180 mEq of Na⁺) per liter for first 8 hours (based on the Parkland Formula). Switch to lactated Ringer's when pH normalizes or at 8 hours. Adjust rate based on urine output.
- Colloid formulas
- Burn budget formula of F.D. Moore: lactated Ringer's 1000–4000 ml + 0.5 normal saline 1200 ml + 7.5% of body weight colloid + 1500–5000 ml D₅W. For second 24 hours, use same formula except for colloid 2.5% of weight.
- Evans formula: normal saline at 1 ml/kg/% TBSA burn + colloid at 1 ml/kg/% TBSA burn. For second 24 hours, give half of first 240 hour requirements + D₅W (dextrose 5% in water) 2000 ml.
- Brooke formula (original): lactated Ringer's at 1.5 ml/kg/% TBSA burn + colloid at 0.5 ml/kg/% TBSA burn. Switch to D₅W 2000 ml for second 24 hours.
- Slater formula: lactated Ringers 2000 ml + fresh-frozen plasma at 75 ml/kg/24 hours. Adjust rate based on urine output.
- Haifa formula: plasma at 1.5 ml/kg/% TBSA burn + lactated Ringer's at 1 ml/kg/% TBSA burn. Adjust rate based on urine output.
- Demling formula: Dextran40 in normal saline at 2 ml/kg/hr for 8 hours. Fresh-frozen plasma at 0.5 ml/kg/hr starting at 8 hours. Lactated Ringer's should be given to maintain urine output.

Figure 6: List of past and current fluid resuscitation formulas [11].

2.2. Task 2: Anthropometric Body Shape Generation

2.2.1. 3D Principal Component Analysis (PCA) of ANSUR II Body Scans

Through a SBIR Phase II project concurrently ongoing with CFDRC and the U.S. Army, "Whole-body Anthropometric Design Models for Protective Equipment Design" with PI Dr. Alex Zhou who is a co-PI on this project, we were able to gain access to 3D body models in the ANSUR II database from Dr. Brian Corner and Dr. Peng Li of the Warfighter Directorate at U.S. Army Natick Soldier Systems Center (NSRDEC). They provided two sets of data (one male and one female), including a mean surface model, ± 3 S.D. (standard deviation from the mean surface) principal shapes for selected principal component or eigenvectors, and variances for each vector, which were all derived from PCA of ANSUR II 3D body scans.

In general, PCA characterizes the variations of body shapes by breaking down each shape into a linear combination of orthonormal component vectors. The component vectors are ordered by their contribution to the variance such that the first component accounts for most of the variance, while the second explains most of the remaining variance after factoring out the first, and so

forth. This approach identifies the correlations between components and reduces the number of anthropometric measurements needed for reconstruction by omitting low variance components [12].

The male and female datasets from NSRDEC were generated from centralized surfaced models, whose origins were all translated to their centroid before calculating PCA. This process eliminated the global translation variances from the PCA. The 3D PCA started with a template body surface model (triangular mesh) fitted to thousands of 3D body scans, which resulted in body models sharing the same triangulation and suitable for PCA. The mean surface model was obtained by averaging all surfaces and deviations from the mean were calculated for each individual model. PCA was then performed to determine all principal values and vectors by computing the covariance matrix of all deviation vectors [12].

For the male dataset, 53 principal component (PC) vectors are needed to account for 99% of variance. For 98% variance, 34 PCs are required. Since no significant shape variation can be observed after the 15th PC, we decided to utilize the 34 male PCs for algorithm and software development, which can be easily extended if more PCs are needed and to the female model as well. It must be noted that there exist pose variations due to arm/leg openness, body tilt left/right or forward/backward captured during the 3D body scanning, which are shown as major shape variations in top 10 PCs. Despite these pose variations, the anthropometry body measurements computed from the PCs are accurate.

2.2.2. Anthropometry Body Features and Landmarks

According to ANSUR II, there are 93 direct and 41 indirect calculated anthropometry body measurements. These measurements are extensive and require trained personnel and specialized equipment like sliding, spreading, Holtain and Poech sliding calipers, and anthropometers to accurately acquire [13]. In the context of a hospital emergency room or even in the combat theater, such detailed body measurements are impractical, too time-consuming and any added benefit to the outcome of the burn patient will most probably be insignificant. As such, we have reduced the number of ANSUR II body measurements to just those that maybe more feasible and practical to acquire. For example, hand and foot widths, and forearm-forearm breath measurements do not contribute significantly to body shape variations. Measurements like vertical trunk circumference, interscye ii and crotch length are impractical to acquire in emergency room setting (Figure 7). More useful measurements include height, limb and torso lengths and circumferences.

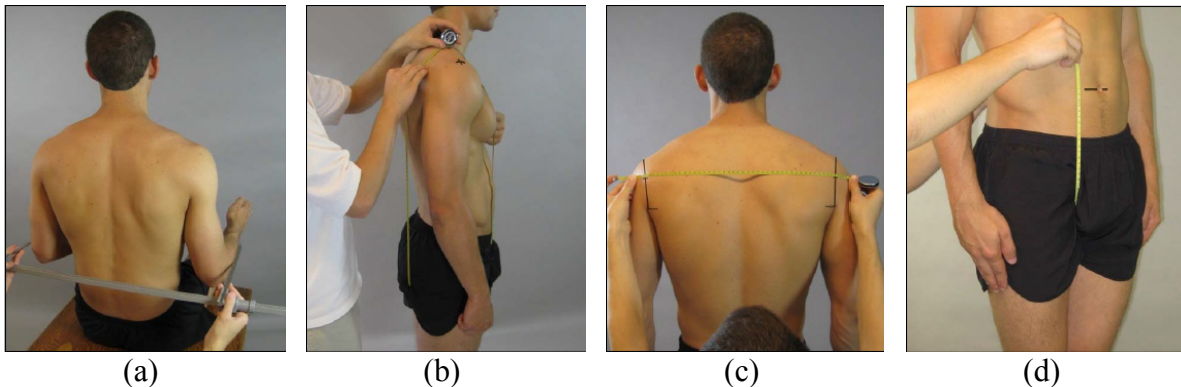


Figure 7: Examples of impractical and insignificant ANSUR II anthropometry measurements eliminated from the body feature list [13] include (a) forearm-forearm breath, (b) vertical trunk circumference, (c) interscye ii, and (d) crotch length.

Additionally, we have added some supplementary measurements that maybe the easiest to acquire. The selected ANSUR II measurements with our additional segment dimensions, collectively called body features, are calculated using body landmarks from ANSUR II and additional supplementary points (Table 1). Weight is different from all other features and is calculated by multiplying the total volume of the model with density. The density for each gender is calibrated such that the average weight calculated falls within the ANSUR II measurement. For male, density is 992.5 kg/m^3 and is 965.0 kg/m^3 for female. The volume of this triangular surface model is computed based on the Gauss divergence theorem. Note that this list of body features can be expanded or even further reduced if desired and will evolve with clinical testing.

Table 1. List of male and female body features selected for their feasibility and practicality to acquire and their measurement type. Male only feature is highlighted.

No.	Body Feature	Source	Measurement Type
1	height	ANSUR II	line
2	weight	ANSUR II	other
3	arm_length_L/R	Supplementary	open_polyline
4	arm_circum_L/R	ANSUR II	slice
5	calf_circum_L/R	ANSUR II	slice
6	chin_nosebridge_length	ANSUR II	line
7	chest_breadth	ANSUR II	line
8	chest_circum	ANSUR II	horizontal_slice
9	chest_depth	ANSUR II	line
10	crotch_height	ANSUR II	line
11	forearm_length_L/R	ANSUR II	line
12	forearm_circum_L/R	ANSUR II	slice
13	foot_length_L/R	ANSUR II	line
14	head_circum	ANSUR II	slice
15	head_breadth	ANSUR II	line
16	hip_breadth	ANSUR II	line
17	hip_circum	ANSUR II	horizontal_slice
18	iliocristale_height_L/R	ANSUR II	line

19	knee_height_midpatella	ANSUR II	line
20	leg_length_L/R	Supplementary	open_polyline
21	neck_circum_AdamsApple	ANSUR II	option_slice
22	shank_length_L/R	ANSUR II	line
23	shoulder_circumference	ANSUR II	horizontal_slice
24	shoulder_depth	Supplementary	line
25	shoulder_width	Supplementary	line
26	standing_eye_height	ANSUR II	line
27	sternum_height	ANSUR II	line
28	thigh_length_L/R	ANSUR II	line
29	thigh_circum_mid_L/R	Supplementary	horizontal_slice
30	thigh_circum_ANSURII_L/R	ANSUR II	horizontal_slice
31	thigh_circum_low_L/R	ANSUR II	horizontal_slice
32	trochanter_height_L/R	ANSUR II	line
33	upperarm_length_L/R	Supplementary	line
34	waist_depth	ANSUR II	line
35	waist_breadth	ANSUR II	line
36	waist_height	ANSUR II	line
*37	waist_front_length	ANSUR II	open_curve
38	waist_circum_omphalion	ANSUR II	horizontal_slice

*Male only.

For the female dataset, 2 body features, head_circum and waist_front_length, are problematic. The 3D body scans of the females captured their hair buns, where the female subjects had their long hair tied up into a bun tucked under a wig cap, which result in inaccurate opisthocranion landmark positioning and therefore head_circum measurements (Figure 8a). This was an unforeseen issue that was unexpected until the ANSUR II female has been provided to us and we had a chance to review the 3D scan. We attempted to correct for the inaccurate back of the mean female head by using a human skull whose size is proportionately adjusted to fit within the front of the mean female. The protruding surface at the back of the head was then smoothed such that it conforms to the shape of the skull (Figure 9a). The inclusion of the hair bun in the mean female mesh results in increases in surface area of about 0.33% to the TBSA and about 5.33% to the head alone. Although the hair bun corrected for the most of the generated female body shapes, there are some cases where the protrusion is still obvious (Figure 9b). To ensure proper correction while not skewing the anthropometry body shape generation, we systematically reviewed the 34 PCs and dropped the ones that had significant effect on the shape of the female head. As a result, 10 PCs were eliminated, all of which are ranked 21st and below. One PC of influence ranked much higher at 4th which makes it a significant component that we cannot eliminate. We therefore computed a new 4th PC by generating a new surface with only the 4th PC set to the maximum 3 S.D. The hair bun protrusion in this new surface was then smoothed (Figure 9c) and the vertices in smoothed surface was subtract from that in the mean to obtain the new 4th PC after accounting for the 3 S.D. In the end, 24 PCs are used for the female dataset. Verification of the accuracy of the PCA generated 3D male and female body features is performed in Section 2.2.4.

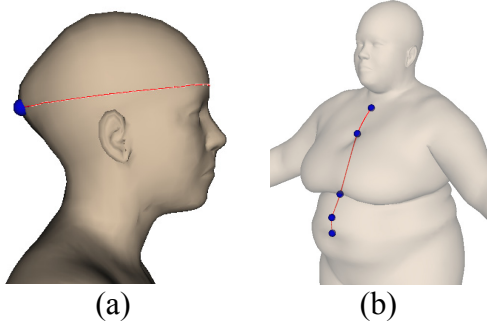


Figure 8: Illustration of problematic body features that includes (a) head_circum and (b) waist_front_length.

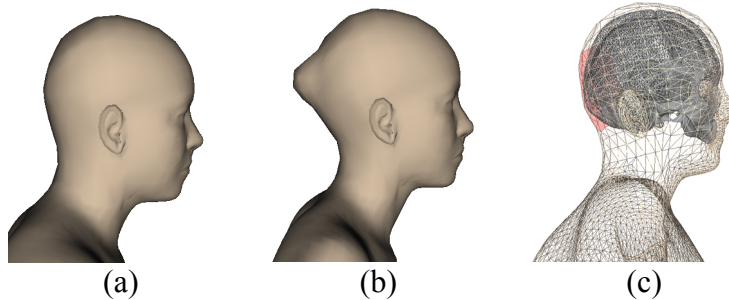


Figure 9: (a) Smoothed back of head to correct for the hair bun in the mean female body surface mesh, (b) protrusion and (c) smoothing areas (highlighted in red) at the back of the head in a generated body surface case.

The other inaccurate female body feature is waist_front_length, which is the surface distance that runs along (from top to bottom) the suprasternale, waist_front_length_2, sternum, waist_front_length_1 and the anterior omphalion landmarks (Figure 8b). Since the female subjects were wearing jogging bras during scanning, these clothing were captured as well and the intermammary clefts are obstructed. Although this measurement is quite useful particularly in abdominally obese individuals since it describes the contour of the abdominal, other body features such as chest_breadth/circum/depth, hip_breadth/circum and waist_depth/breadth/circum_omphalion serves to describe abdominal size as well. As such, waist_front_length can be dropped for the female.

The landmarks used are based on ANSUR II plus supplementary ones. The latter ones are used for direct body feature measurement and indirect calculations to facilitate such measurements such as determinations of floor plane and orthogonal axes. Figure 10 shows all 135 landmarks assigned on the 3D surface mesh of a mean ANSUR II male and female body. The coordinates of each landmark only need to be recorded once for the mean surface model and they are automatically translated to other synthesized models. The descriptions of the landmark locations are given in Table 2, with ‘L’ in the name referring to the left landmark and ‘R’ to the right.

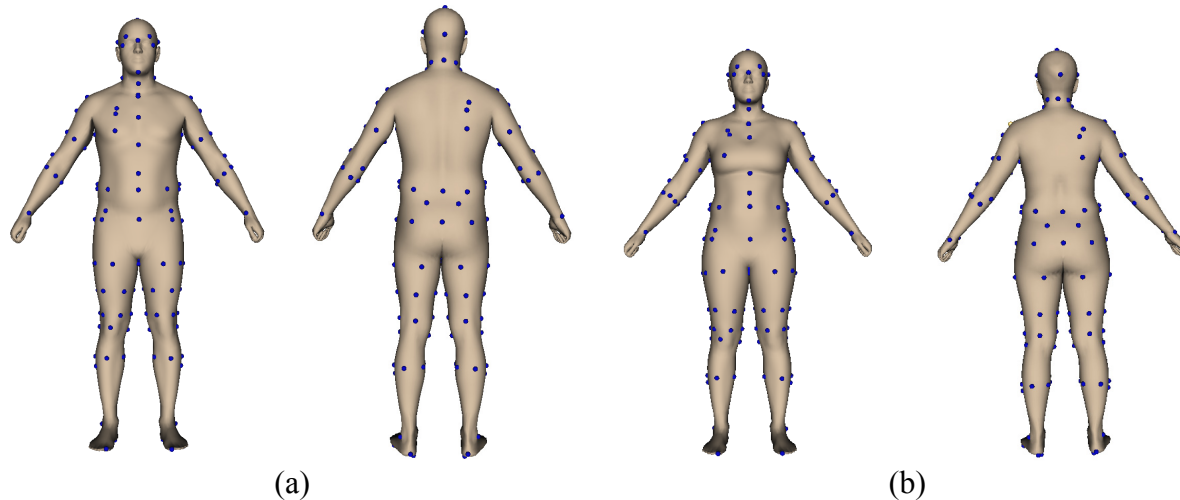
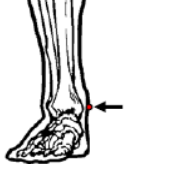
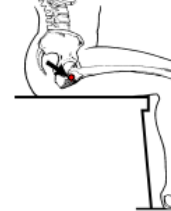
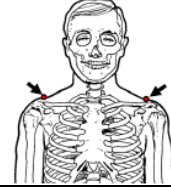
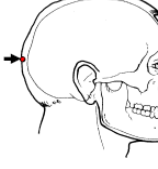
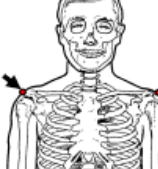
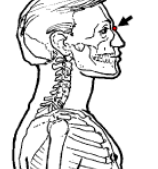
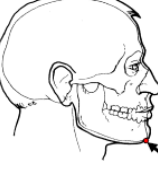
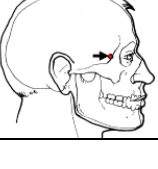
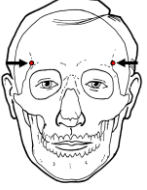
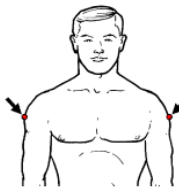
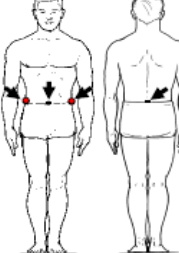


Figure 10: Front and back view of the all the landmarks (blue spheres) on the (a) male and (b) female body.

Table 2. Description of the all body landmark locations [13]

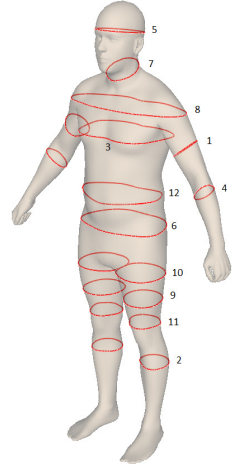
Landmark	Location
FloorFootL/R	Bottom of foot, anywhere that touches the floor.
AnkLatL/R	Lateral malleolus. 
AnkMedL/R	Medial malleolus. 
KneeMedL/R	Medial of two points between which knee flexion axis passes through skin.
KneeLatL/R	Lateral of two points between which knee flexion axis passes through skin.
LPSI / RPSI	Posterior superior iliac spine.
LASI / RASI	Anterior superior iliac spine.
TrochanterL/R	Greater trochanter. 
Sternum	Xiphoid process of sternum.
Clavicle	Jugular notch where clavicle meets sternum. 

Suprasternale	Inferior point of the jugular notch of the sternum (top of the breastbone).	
HeadTop	Approximate highest point of head.	
ElbowAntL/R	Lateral epicondyle.	
ElbowPostL/R	Medial epicondyle.	
WristAntL/R	Medial side of wrist where joint axis passes through skin.	
WristPostL/R	Lateral side of wrist where joint axis passes through skin.	
ThighL/R	Lateral side of thigh, on a straight line with knee and hip joint centers.	
ShankL/R	Lateral side of shank, on a straight line with knee and ankle joint centers.	
ArmL/R	On side of arm, placed on line between shoulder and elbow joint centers.	
Torso	Placed anywhere on torso segment, away from centerline.	
Lumbar	Placed anywhere on lumbar segment, away from centerline.	
Opisthocranion	Posterior point on the back of the head.	
AcromionL/R	Tip of the shoulder.	
Sellion	Point of the deepest depression of the nasal bones at the top of the nose.	
Menton	Inferior point of the mandible in the midsagittal plane (bottom of the chin).	
EctoorbitaleL R	Posterior point on the frontal process of the zygomatic bone at the level of the outer corner of the eye.	

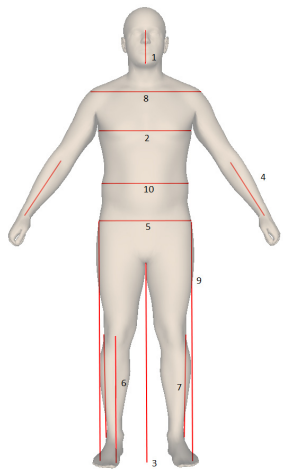
FrontotemporaleL/R	Point of deepest indentation of the temporal crest of the frontal bone above the browridges.	
DeltoidPointL/R	Midpoint of the left and right deltoid muscles.	
MidDeltoidAnt/Post	Midpoint of the anterior and posterior deltoid muscles.	
ChestPointAntR	Most anterior right point on the chest.	
IliocristaleL/R	Highest palpable point of the right and left iliac crests of the pelvis, one-half the distance between the anterior superior iliac and posterior superior iliac spines.	
OmphalionAnt/Post/L/R	Level at the center of the navel.	
MidpatellaR	Anterior point halfway between the top and bottom of the patella (the kneecap).	
WaistCirc1,3,7	At omphalion height around waist.	
HipCirc1-6	At height of TrochanterL and TrochanterR around pelvis.	

ThighLHighCirc1-5/ ThighRHighCirc1-5	Around the lowest point of the lowest furrow or crease at the juncture of the buttock and thigh.	
ThighLCirc1-4 / ThighRCirc1-4	Around level of thigh that is between ThighHighCirc and ThighLowCirc.	
ThighLLowCirc1-5/ ThighRLowCirc1	Around the highest point of the knee at the thigh.	
ArmLCirc1-3 / ArmRCirc1-3	Around biggest part of the arm.	
CalfLCirc1-5 / CalfRCirc1-5	Around biggest part of the calf.	
NeckCirc1-3/ NeckCircA1-2/ NeckCircB1-2	Around the neck, to form a smooth circumference with the anterior and lateral neck landmarks from ANSUR II.	
AdamsApple	Adam's apple.	
Crotch	Point at the level of the lower edge of the pubis bone of the os coxa.	
ForearmLCirc1-6/ ForearmRCirc1-6	Around biggest part of the forearm.	
ChestL/R	Widest points along the chest.	
HeelL/R	Posterior point on the heel of the foot.	
ToeL/R	The tip of the first or second toe of the right foot, whichever is longer.	
EurionL/R	Highest point of the parietal eminence.	

Typical geometrical functions, such as the length of a straight line, an open or closed poly line or curve, are used to connect these landmarks. The straight lines connect two points and the poly lines connect multiple points with straight lines. The curves fit polynomial equations through the points and are typically used for circumferences or curved lines. For special circumferences, the body surface mesh is sliced either in the horizontal plane or at arbitrary angles depending on the referenced landmarks, and the intersection of the plane and the body surface forms the body circumference (Figure 11). Details of the landmarks and body features in the GUI are highlighted in Section 2.6.1.



1. arm_circum_L/R
2. calf_circum_L/R
3. chest_circum
4. forearm_circum_L/R
5. head_circum
6. hip_circum
7. neck_circum_AdamsApple
8. shoulder_circumference
9. thigh_circum_mid_L/R
10. thigh_circum_ANSURII_L/R
11. thigh_circum_low_L/R
12. waist_circum_omphalion



1. chin_nosebridge_length
2. chest_breadth
3. crotch_height
4. forearm_length_L/R
5. hip_breadth
6. knee_height_midpatella
7. shank_length_L/R
8. shoulder_width
9. trochanter_height_L/R
10. waist_breadth



1. chest_depth
2. shoulder_depth
3. standing_eye_height
4. sternum_height
5. upperarm_length_L/R
6. waist_depth
7. waist_height

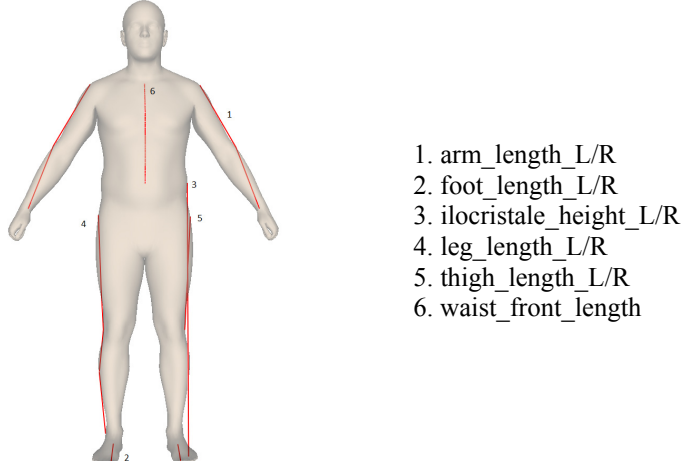


Figure 11: Body feature measurements (red lines).

2.2.3. Relation Between 3D PCA and Traditional Measurement

The technique of PCA was used to characterize the variations of body shapes by breaking down each shape into a linear combination of principal component vectors. Key components identified with 3D PCA can be related to each other but may not be directly correlated to traditional anthropometric parameters. Blanz and Vetter [14] introduced a linear regression method to link the PCs to any single anthropometric parameter. This linear mapping between multiple anthropometry body features and 3D PCA weights allows reconstruction of 3D human models with direct anthropometric controls [12]. Any combination of the 38 body features, identified in Table 1, can be selected based on their measurability and used for inverse mapping. For simplicity, height, weight and waist circumferences are set as the initial default feature values in our software GUI. All other body features can also be selected. Details of this capability in GUI are highlighted in Section 2.6.1.

2.2.4. Feature Comparisons between 3D PCA Models and Measurements

To verify the accuracy of the PCA generated 3D body features, these values were compared to the traditional measurements from the ANSUR II database, which were collected from 4082 male subjects (Table 3). Body features that are from the ANSUR II database were analyzed. The mean and S.D. of the ANSUR II measurements were extracted from the official report [13] and the measurements from the 4082 virtually generated male body shapes using the normally distributed random generation method on the PCA values were calculated. For the female, 1986 virtually generated random female body shapes were used (Table 3). All correspondences agree very well with the physical measurements with the sole exception of chest_breadth. The mean and S.D. comparison is also presented graphically in Figure 12.

Table 3. Comparison between 3D features and their corresponding traditional measurements for male and female. Units are in meters unless otherwise indicated.

Feature	ANSUR II	PCA model male		ANSUR II male		% Error	PCA model female		ANSUR II female		% Error
		Mean	S.D.	Mean	S.D.		Mean	S.D.	Mean	S.D.	
Age (years)				30.2	8.8				28.94	8.33	
height	STATURE	1.759	0.08	1.756	0.069	0.17	1.6292	0.0643	1.629	0.0642	0.042
weight	WEIGHT	85.25	14.62	85.52	14.22	-0.32	68.0	11.1	67.76	11.0	0.320
arm_circum	BICEPS CIRCUMFERENCE, FLEXED	0.326	0.0327	0.3581	0.0346	-8.96	0.304	0.0316	0.3056	0.0308	-0.607
calf_circum	CALF CIRCUMFERENCE	0.398	0.0329	0.392	0.0297	1.54	0.3711	0.0270	0.3733	0.0285	-0.590
chin_nosebridge_length	MENTON- SELLION LENGTH	0.126	0.00388	0.123	0.007	2.29	0.1099	0.0032	0.1131	0.00610	-2.834
chest_breadth	CHEST BREADTH	0.351	0.034	0.289	0.0183	21.66	0.3150	0.0228	0.2693	0.0186	16.988
chest_circum	CHEST CIRCUMFERENCE	1.081	0.0958	1.059	0.0874	1.85	0.995	0.108	0.9469	0.0827	5.117
chest_depth	CHEST DEPTH	0.258	0.0269	0.254	0.0262	1.31	0.2421	0.0248	0.2474	0.0273	-2.153
crotch_height	CROTCH HEIGHT	0.77	0.0492	0.846	0.0465	-8.76	0.7372	0.0439	0.7823	0.0446	-5.760
forearm_circum	FOREARM CIRCUMFERENCE, FLEXED	0.289	0.0232	0.2679	0.0154	-6.76	0.2321	0.0128	0.2413	0.0152	-3.798
forearm_length	RADIALE- STYLIUM LENGTH	0.257	0.0156	0.3101	0.022	-4.03	0.2504	0.0214	0.2641	0.0185	-5.194
foot_length	FOOT LENGTH	0.288	0.0188	0.2712	0.0131	6.37	0.2532	0.0140	0.2463	0.0124	2.789
head_circum	HEAD CIRCUMFERENCE	0.584	0.0152	0.574	0.016	1.83	0.5602	0.0176	0.5611	0.0194	-0.169
hip_breadth	HIP BREADTH	0.359	0.0224	0.346	0.024	3.63	0.3608	0.0243	0.3538	0.0267	1.972
hip_circum	BUTTOCK CIRCUMFERENCE	0.998	0.0972	1.02	0.077	-2.52	0.995	0.100	1.021	0.0759	-2.539
iliocristale_height	ILIOCRISTALE HEIGHT	1.056	0.0583	1.062	0.052	-0.38	0.9993	0.0493	0.9957	0.0497	0.364
knee_height_midpatella	KNEE HEIGHT, MIDPATELLA	0.489	0.0297	0.488	0.028	0.38	0.4476	0.0243	0.4490	0.026	-0.307
neck_circum_AdamsApple	NECK CIRCUMFERENCE	0.407	0.0248	0.398	0.026	2.11	0.3458	0.0230	0.3298	0.0192	4.846
shank_length	CALF LINK	0.415	0.0259	0.4188	0.0246	-0.58	0.3893	0.0218	0.4032	0.0259	-3.445
shoulder_circumference	SHOULDER CIRCUMFERENCE	1.192	0.135	1.179	0.0636	0.74	1.005	0.117	1.028	0.0529	-2.273
standing_eye_height	EYE HEIGHT	1.633	0.0796	1.642	0.0665	-0.34	1.5144	0.0628	1.520	0.0617	-0.334

sternum_height	SUPRASTERNALE HEIGHT	1.439	0.07188	1.439	0.0612	0.15	1.3218	0.0573	1.330	0.0572	-0.593
thigh_length	THIGH LINK	0.446	0.02498	0.4093	0.0284	9.24	0.4091	0.0219	0.3794	0.024	7.828
thigh_circum_ANSURII	THIGH CIRCUMFERENCE	0.6159	0.055395	0.625	0.058	-1.67	0.6374	0.0820	0.6161	0.0558	3.453
thigh_circum_low	LOWER THIGH CIRCUMFERENCE	0.4204	0.03389	0.4093	0.0319	2.62	0.4137	0.0345	0.4007	0.0352	3.249
trochanterL_height	TROCHANTERION HEIGHT	0.9254	0.05329	0.901	0.0492	2.94	0.8500	0.0451	0.8454	0.0447	0.546
waist_depth	WAIST DEPTH	0.24535	0.03266	0.238	0.0347	2.69	0.2240	0.0291	0.2130	0.0314	5.163
waist_breadth	WAIST BREADTH	0.3376	0.03434	0.326	0.0347	3.32	0.3147	0.0286	0.2999	0.033	4.923
waist_height	WAIST HEIGHT	1.047	0.05897	1.056	0.0522	-0.61	0.9796	0.0476	0.9801	0.0500	-0.051
waist_front_length	WAIST FRONT LENGTH, SITTING	0.39945	0.02522	0.388	0.0293	2.94	-	-	-	-	-
waist_circum_omphalion	WAIST CIRCUMFERENCE	0.9358	0.1055	0.941	0.112	-0.83	0.843	0.135	0.8609	0.0999	-2.136

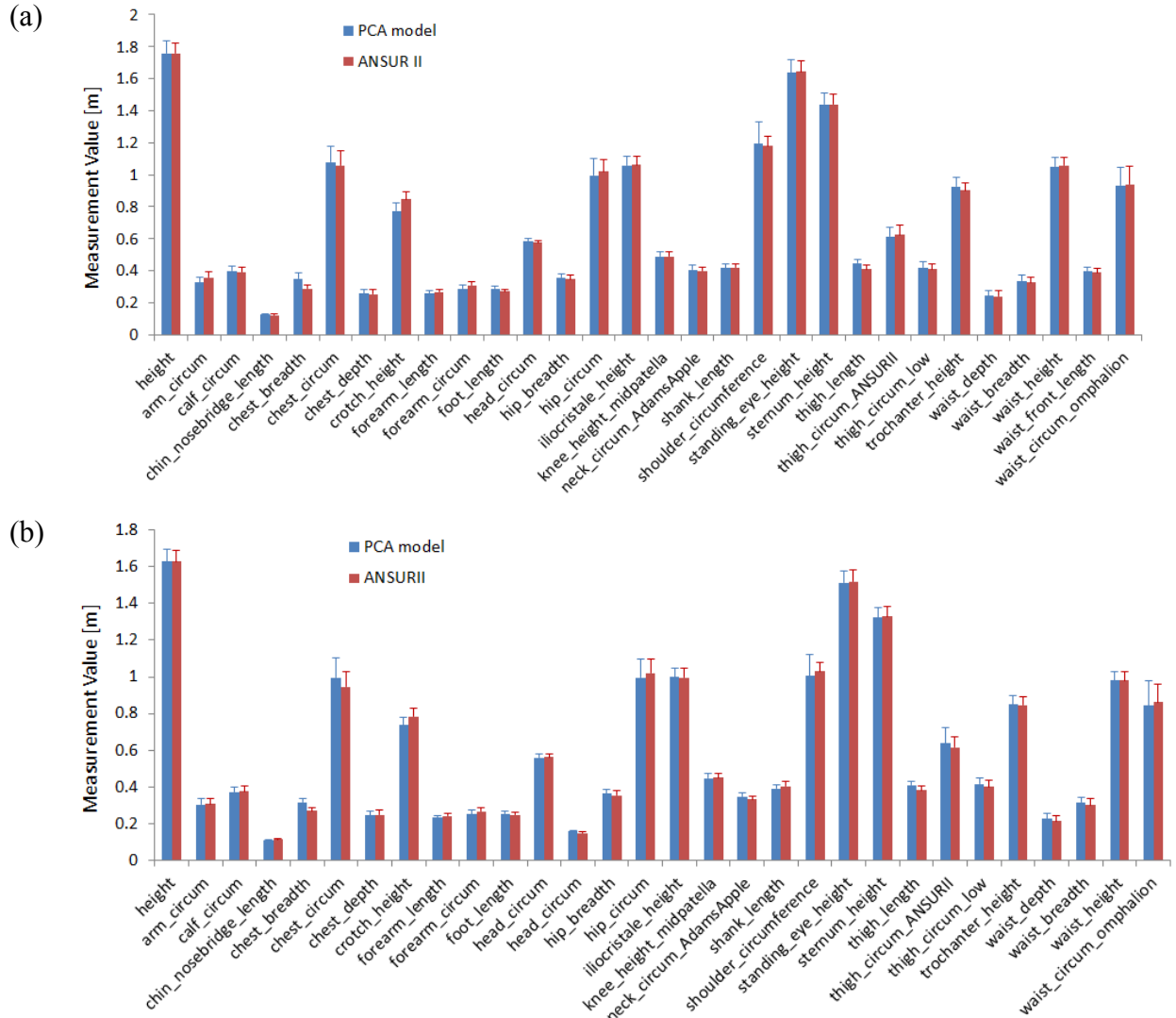


Figure 12. Comparison between 3D features and their corresponding traditional measurements for (a) male and (b) female.

Chest_breadth was overestimated on average by 21.4% for the male and 16.99% for the female. The landmarks used for the calculations were at the correct height as the actual ANSURII landmark was used. The difference is however likely because in the ANSURII measurement the tissue is compressed firmly to ensure contact with the ribcage. The error in the calculation therefore depends on the amount of adipose tissue at the chest breadth height. Also, during scanning, the arms are open (Figure 13b), which stretches some upper torso muscles and could artificially increase the virtual measurement of chest breadth. It would be difficult to adjust for this in the feature calculations. However, if needed, this discrepancy can be compensated by adjusting the user input of this specific feature within the software based on the average error such that proper virtual number is fed to the algorithm. In Figure 13 below, the two left images are extracted from ANSURII reports [15], [16] and the rightmost image is a snapshot from our Anthropometry software tool.

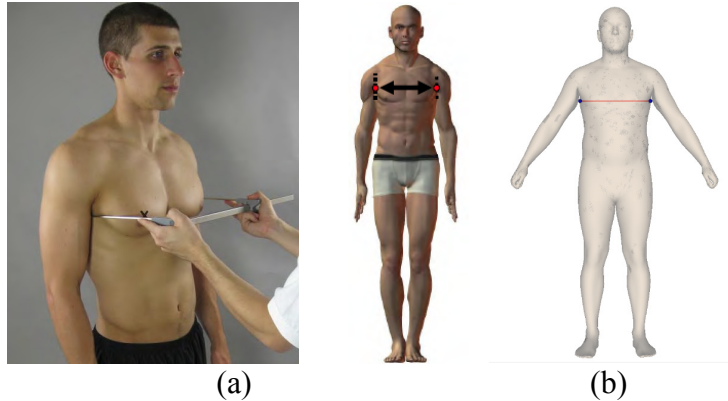


Figure 13. Measurement of chest_breadth as defined in (a) ANSUR II and (b) computed in our Anthropometry software tool.

2.3. Task 3: Cutaneous Functional Unit Classification of the Anthropometry Models

Despite the close relationship between burn treatment and outcomes with %TBSA, there is still some disparity between burn scar contracture (BSC) or joint limitations in range of motion (ROM) with %TBSA [17]. BSC are developed due to the replacement of naturally pliable skin with a more inelastic scar tissue after a second or third degree burn. This tightening of the skin limits the ROM of joints, resulting in deformity, impairment and disability. To aid in burn rehabilitation and surgical planning in escharotomies, Richard et al. [17] identified cutaneous functional units (CFU), which are fields of skin that are involved in the range of motion at joints and are associated with the areas that have a tendency to develop BSC. CFU was also found to be a better indicator of BSC than %TBSA and may offer a more accurate prognosis [18].

As such, the mean surface mesh male and female models were classified into CFU according to the schema developed by Richard et al. [2]. It is a hierarchical decomposition of the human body such that each body part is broken down into an ordered numerical system. The main body segments are divided according to the Rules-of-Nines and assigned a global number of increasing value from head, caudally to the feet. Anterior and posterior distinctions are defined by even and odd numbers, respectively (3rd digit). The 4th digit is for proximal with an even number and distal with an odd number, and so on. Left and right sides of the body are also distinguished by odd and even numbers, respectively.

Figure 14 illustrates the CFU classifications according to our interpretations on the mean male body, where each CFU is assigned a distinct color. The CFU definitions are stored in a comma separated value (CSV) file, which consists of each CFU code, its name and a list of triangle indices to the surface mesh that belongs to that CFU. The CSV file can be modified by other users according their own definitions. However, if details of this file need not be altered, our software tool will also read in a non-modifiable binary form of the CSV file. Our tool will automatically convert the ASCII CSV file to binary form if one does not exist. This binary file can be shared instead of the ASCII version. If both forms are present, preference will be given to the binary version for reading. Morphing the body shape in real-time preserves the CFUs (Figure 15). Figure 16a, b and c illustrates the same CFU classifications on the mean female body, along

with preserved CFUs in different morphed views (Figure 16d, e, and f). Details of the CFU are described in Section 2.6.2.

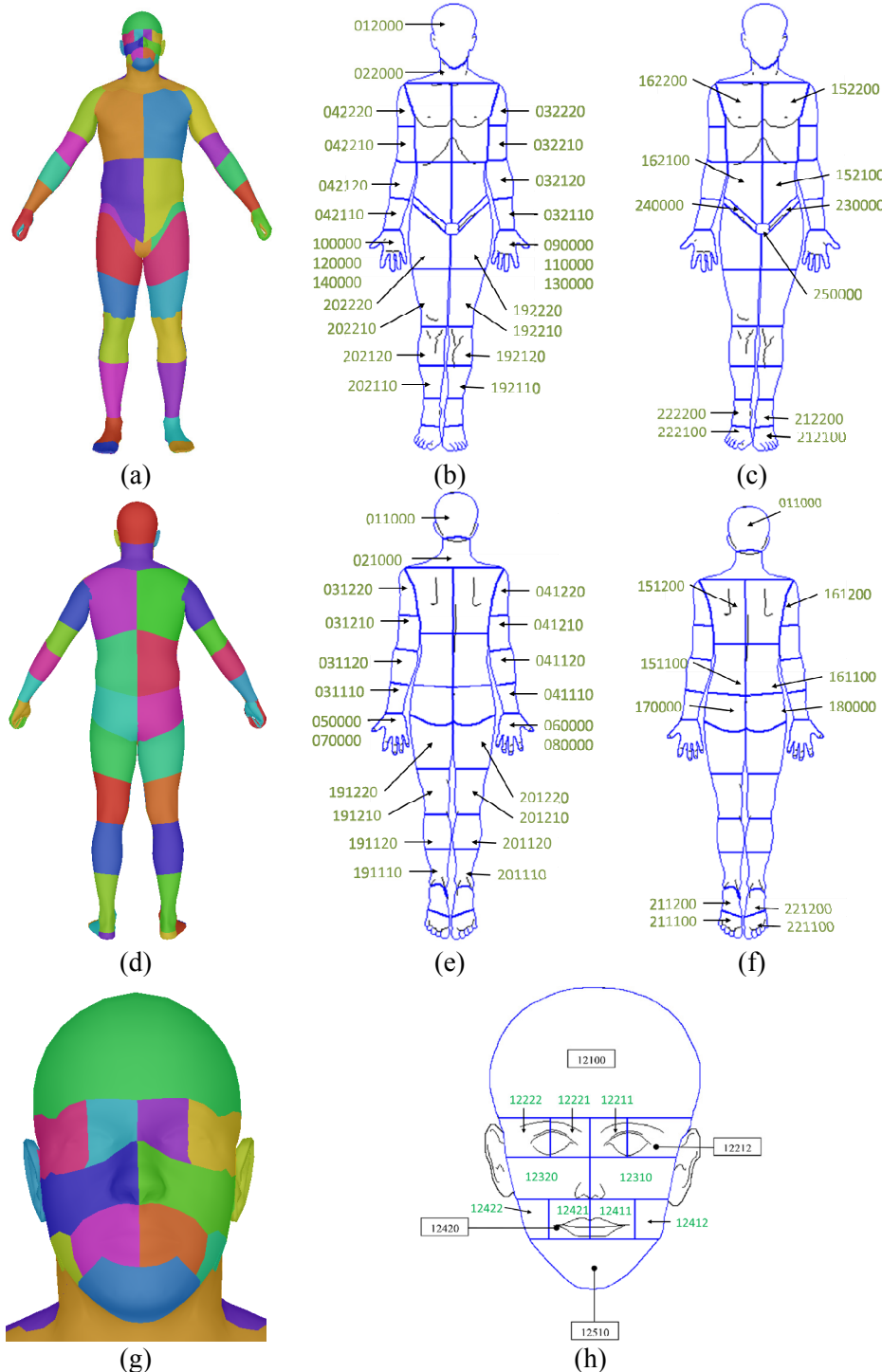


Figure 14. CFDRC's CFU classification based on the schema developed by Richard et al. [2] on the mean male body. (a) Front view of the colored CFUs on the mean male 3D body, and (b) and (c) are the corresponding CFDRC's CFU definitions in the front. (d) Back view of the colored CFUs on the mean male 3D body, and (e) and (f) are the corresponding

CFDRC's CFU definitions in the back. (g) Colored CFU classification of the mean male head corresponds to (h) CFDRC's CFU definitions.

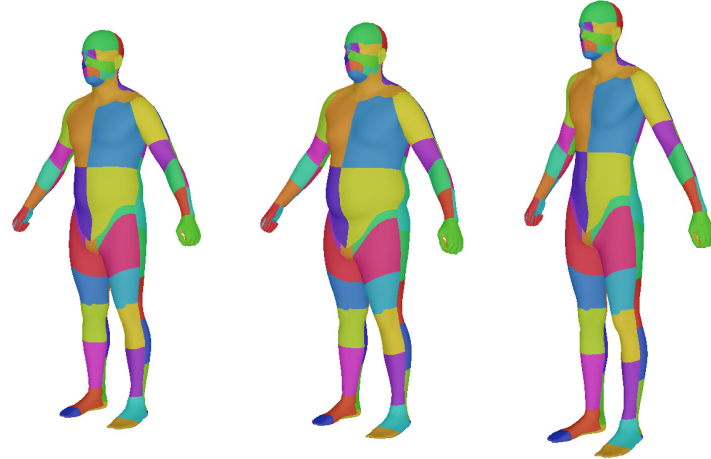
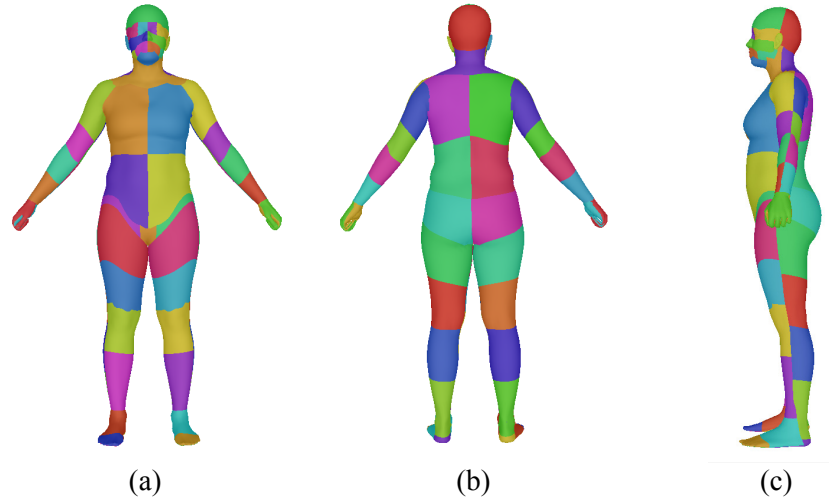


Figure 15. The CFU classification follows the morphing of the male body shapes.



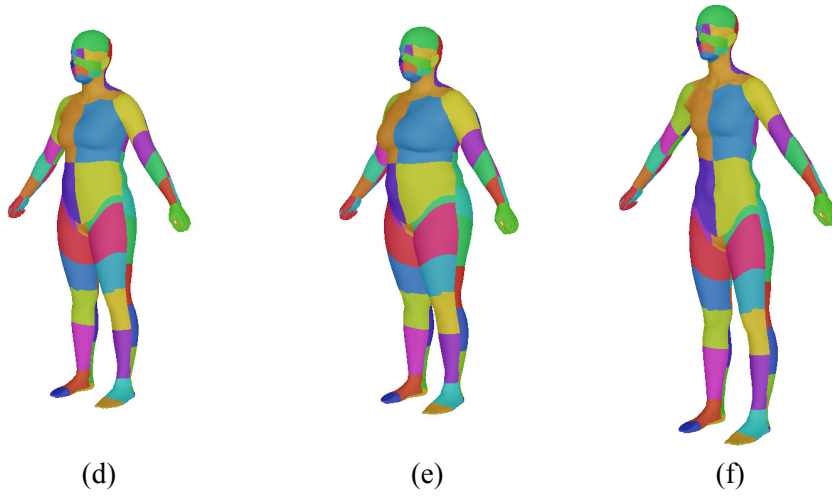


Figure 16. The same CFU classification schema was applied to the mean female body with the (a) front, (b) and (c) side views. This classification also follows the morphing of the female body shapes shown in (d), (e) and (f).

In the CFU definitions we created, the CFU classifications in the hands are absent since the hands from the ANSUR II dataset are closed or in a fist, making the demarcation of the palms difficult. Each hand accounts for only about 1% of TBSA, hence the Rule of Palms, but burns to hands are ranked among the 3 most frequent sites of BSC deformity and the functionality of hands is a significant determinant in the quality of life in burn survivors [19]. Therefore, hands require further software specialization and development more suitable in a lengthier Phase II where the fingers can be opened up by adding articulation to the finger, thereby allowing a more refined classification. In the meantime, the CFU definitions for the front and back of the hands were duplicated. In essence, for the back of the left hand, the main CFU codes, 050000 and 070000, both represent the same surface of the mesh, as do 060000 and 080000 for the back of the right hand. For the front of the right hand, 100000, 120000 and 140000 share the same surface and likewise for the front of the left hand with 090000, 110000, 130000.

2.4. Task 4: Develop Model Surface Demarcation Tools

A mesh surface demarcation tool that involves surface painting using a circle brush was developed, along with the capability to erase the selected surface (Figure 17). The size of the circle brush can be adjusted for demarcations based on different burn severity as well as amputation with different highlighted colors (Figure 17). Details of this capability are illustrated in Section 2.6.3. This capability can not only be used to demarcate burn areas, but was also used for defining surfaces in CFU classification.

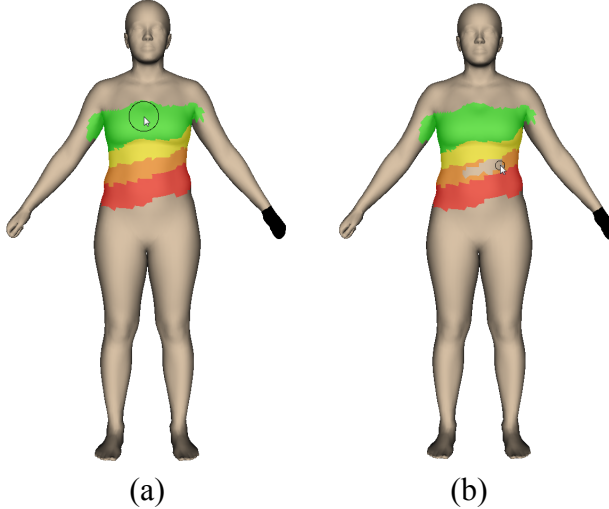


Figure 17. Mesh surface demarcation tool with (a) addition using a larger sized circle brush and (b) erasing with a smaller sized circle brush. Different burn severity (full (red), deep (orange), partial (yellow) and superficial (green)) and amputation (black) demarcations are color coded.

The workflow for our burn injury assessment tool intends for the anthropometry parameters of the patient to be entered to create the virtual 3D patient model prior to burn demarcation. Our tool is also flexible enough for the burn demarcations to morph with the full body surface in real-time (Figure 23). This capability allows %TBSA and thereby fluid recommendations to be determined quickly on an approximate 3D patient model by limited anthropometry parameters, such as height and weight. More detailed anthropometry measurements can be subsequently acquired and entered into our tool for a more accurate %TBSA and fluid recommendations.

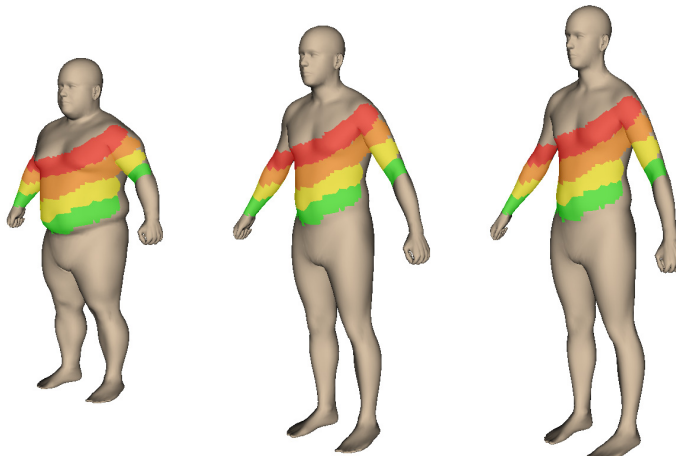


Figure 18. Different demarcated burn severity (full burn (red), deep burn (orange), partial burn (yellow) and superficial burn (green)) surfaces morphs with the full body surface in real-time.

2.5. Task 5: Calculation and Validation of Burn Surface Area

The CFUs are organized in a hierarchical format. Lower level CFUs contain triangle indices from the mesh they belong to, while higher level CFUs may not directly have such information but they contain the lower level CFUs with the information. On initialization of the program, the surface areas for the lower level CFUs are calculated by summing the areas of all the triangles defined for that CFU. For higher level CFUs, areas in each lower level CFU are added up in order. As a result, each CFU, regardless of rank, has a surface area value. This enables %TBSA calculations for each CFU to be calculated directly.

After demarcation, the triangles selected by the demarcation tool for each burn severity are related to the CFUs based on triangle index. For each CFU, the demarcated surface area, if present, is then computed by again summing the highlighted triangles for each burn severity. Finally, the percentage burn to each CFU is calculated by simply dividing the demarcated area by the CFU area already determined. Both burn surface areas in cm^2 and as percentage of its CFU and TBSA are reported. To account for any possible amputations that could change the patient's weight, the volume of the amputated geometry is subtracted from the total body volume to determine the adjust body volume to multiply with human density for weight calculation. Additionally, the surface areas to CFUs and thereby TBSA are adjusted for the amputated surface areas. With these modifications to %TBSA and weight, the standard fluid resuscitation formulas (Parkland and Brooke) are used to calculate the required fluids for amputees. Details of the burn area reporting are described in Section 2.6.4.

The demarcated burn surface area from our software tool was verified by comparing the surface areas calculated to other methods of estimating human body surface areas (BSA). Various BSA formulas have been developed to calculate surface area using easily measured height and weight (Table 4). The BSA calculated are most commonly used to determine medication doses, such as chemotherapy, since it is a better indicator of metabolic mass than body weight as it is less affected by abnormal adipose mass.

Table 4: Human body surface area formulas.

Formula	BSA (m^2)
Mosteller [20]	$\sqrt{\frac{\text{height(m)} \times \text{weight(kg)}}{3600}}$
DuBois & DuBois [21]	$0.20247 \times \text{height(m)}^{0.725} \times \text{weight(kg)}^{0.425}$
Haycock [22]	$0.024265 \times \text{height(m)}^{0.3964} \times \text{weight(kg)}^{0.5378}$
Gehan & George [23]	$0.0235 \times \text{height(m)}^{0.42246} \times \text{weight(kg)}^{0.51456}$

The height, weight and TBSA measurements from 1000 virtually generated male and female body shapes using the normally distributed random generation method on the 34 and 24 principal component analysis values, respectively, were produced. For the male sample set, the height ranged from 1.5 m to 2.0 m and weight from 43.8 kg to 137 kg. The female sample set had height ranging from 1.4 m to 1.8 m and weight from 39.2 kg to 105 kg. The height and weight data from each model were then used to calculate the BSA given using the above formulas. The

absolute error between the formula based BSAs and TBSA from our software for each gender were calculated (Figure 19). For the male, the largest average absolute error is 0.11 m^2 (relative error of 5.0%) using the DuBois & DuBois formula, while the smallest is 0.070 m^2 (relative error of 3.4%) with the Haycock formula. For the female, the largest average absolute error is 0.11 m^2 (relative error of 6.0%) using the DuBois & DuBois formula, while the smallest is 0.073 m^2 (relative error of 4.0%) with the Gehan & George formula. Since these formulas are derived from regression analyses of only 2 anthropometric parameters (height and weight) of large population datasets, relatively significant deviations are expected.

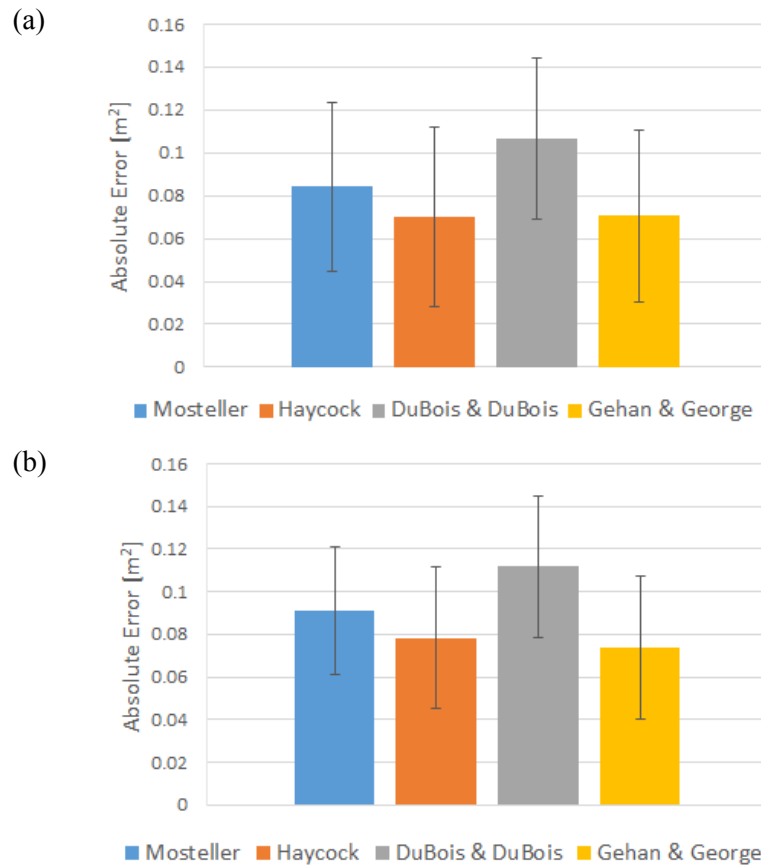


Figure 19: Average absolute errors between TBSAs calculated using our software tool and the formula based BSAs for the 1000 randomly generated (a) male and (b) female bodies. The error bars denote 1 standard deviation from the mean.

Additionally, the Rule-of-Nines method of determining surface area was used for comparison with %TBSA calculated with our software tool. The Rule-of-Nines is a method currently used by some emergency response teams to estimate the amount of surface area burned on a patient. This approach divides the generic body diagram into segments, each representing about 9% of the TBSA [9]. %TBSA is thereby determined by estimating the burn areas in each segment and summing the percentages up. Of the 1000 randomly generated male models used previously to determine the TBSA, %TBSA to whole arms, legs, torso, groin, and head, as defined by Rule-of-Nines method, were produced and compared to the Rule-of-Nines estimates (Figure 20). The average %TBSA calculations from our software tool are in close agreement with the Rule-of-

Nines estimates for the whole body segments since the latter is a prediction based on the average human body. The range of the %TBSA calculated with our tool showed greater variability in the torso region. These discrepancies in %TBSA, although small individually, may become significant when they are summed up for burns in multiple body segments. Furthermore, for burn areas that do not fit perfectly within these defined body segments, the user would have to estimate %TBSA for the Rule-of-Nines method, thereby potentially adding to the discrepancies.

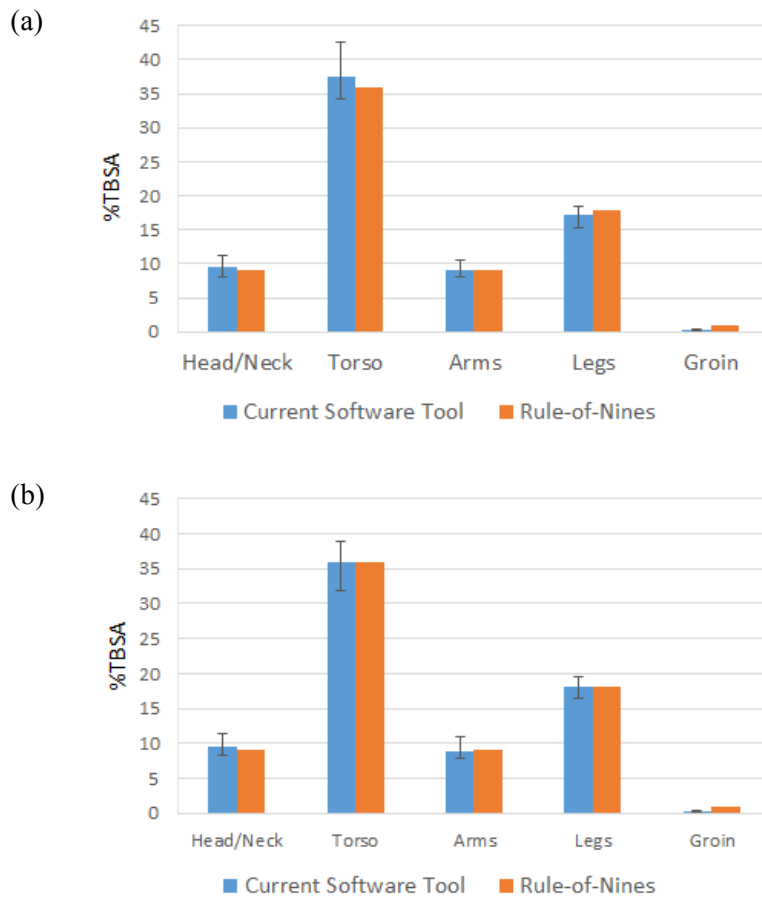


Figure 20: %TBSA for head/neck, torso, arms, legs, and groin calculated using our software tool and Rule-of-Nines method for the 1000 randomly generated (a) male and (b) female bodies. The error bars denote the range of the %TBSA values.

2.6. Task 6: GUI Design and Development

2.6.1. Anthropometric Body Generation

Upon initialization of the software tool, the male model is automatically loaded by default. The user can input the patient's biological information, including first and last name, social security number, date of birth, gender, blood type, time and date of incident, and type of burn (thermal, chemical, electrical, radiation and friction) (Figure 21). Switching genders will automatically update the 3D model and anthropometry feature list. The list of 53 and 51 anthropometry

features for the male and female, respectively, is simplified to be automatically linked to height, weight and waist circumferences as the initial default feature values. This links the traditional 1D anthropometry body feature measurements to 3D principal components using inverse linear mapping. Pressing on the “Show Advanced Features” button reveals the full anthropometry feature lists from which the user must first select the feature(s) of interest and then activate the links between selected features and PCs. Multiple body features can be selected depending on which anthropometry measurement is practical to acquire for the burn patient by pressing “Ctrl” while selecting with the mouse. The user then right clicks to choose “link features to PC” (Figure 22). The inverse mapping between the selected body features and 3D PCA weights will be computed and slide bars will show up for these selected features. The user can then adjust the slide bar to change the individual selected body features interactively, while the PCs and body shape are updated simultaneously.

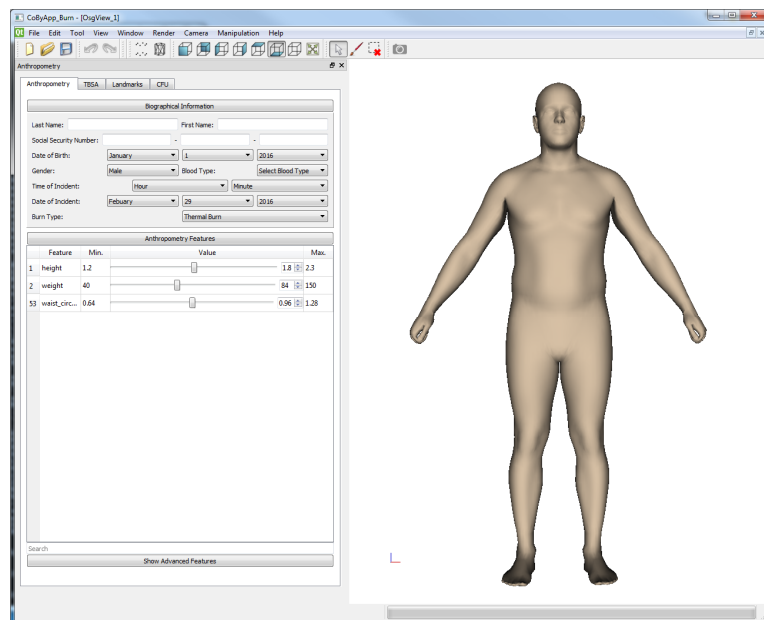


Figure 21. Screenshot of the software tool upon initialization with the male model automatically loaded and the biographical information and default anthropometry features (height, weight and waist circumference) displayed for the user to input.

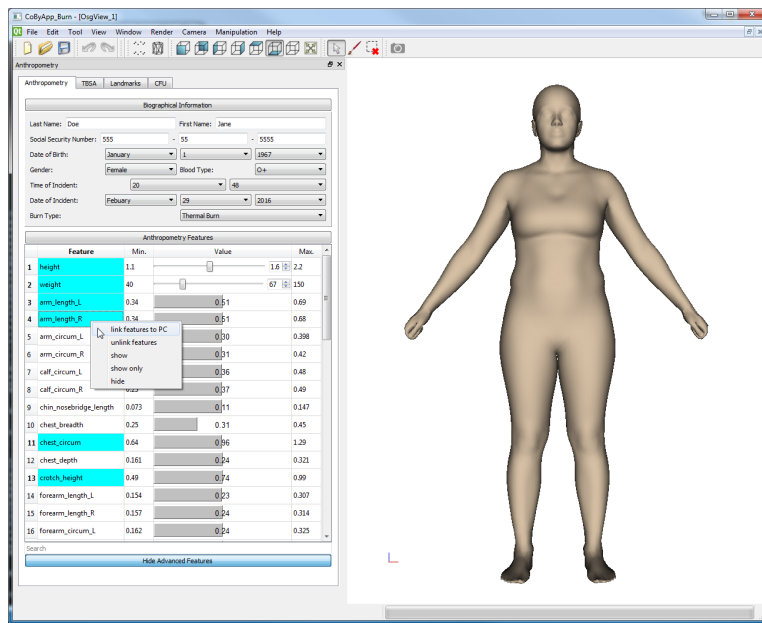
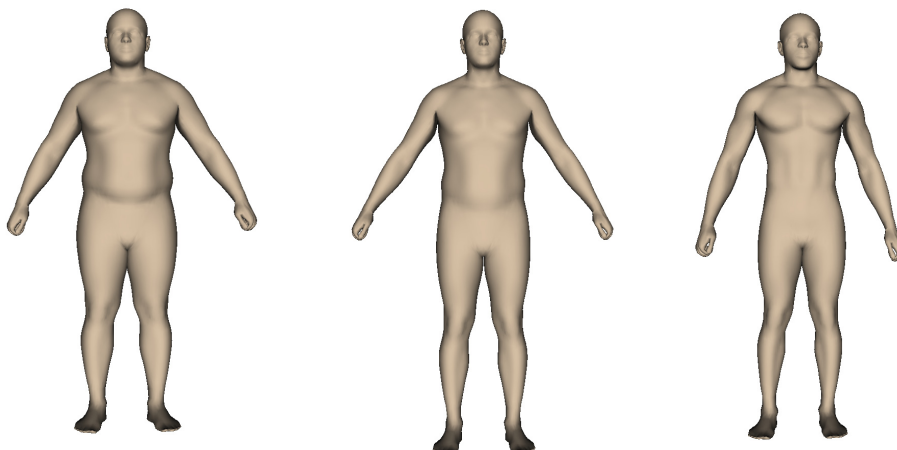


Figure 22. Screenshot of the tool with female gender selected and advance anthropometry features selected for the user to input.

In Figure 23, examples of generated male and female body shapes from user manipulation of the selected body features are shown. The user has the choice to specify the limits for any features or allow the program to automatically compute them. The limits can be specified beyond typical normal ranges if desired, which allows the user to synthesize body shapes that are outside the boundary of the given database.

(a)



(b)

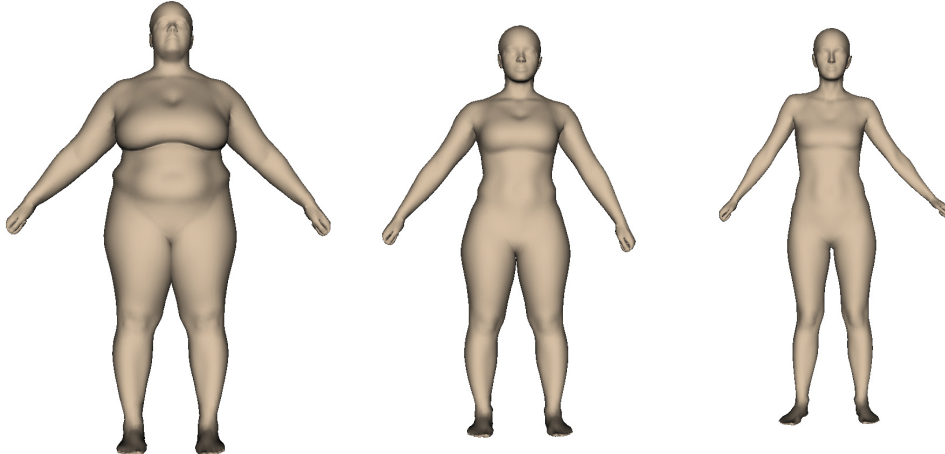


Figure 23. Examples of arbitrary (a) male and (b) anthropometric models.

There is also a Landmarks tab that lists all the surface landmarks assigned to the body surface, which are used to calculate body feature values. The display of these landmarks can be turned on or off by clicking the visible button for all points or just those of interest. Upon selection of each landmark, positional information of that point is displayed on the right panel and can be adjusted if necessary (Figure 24). For the typical end-user, this tab is not usually needed. However, it may be useful for advance users who wish to add or modify landmarks for customized body features.

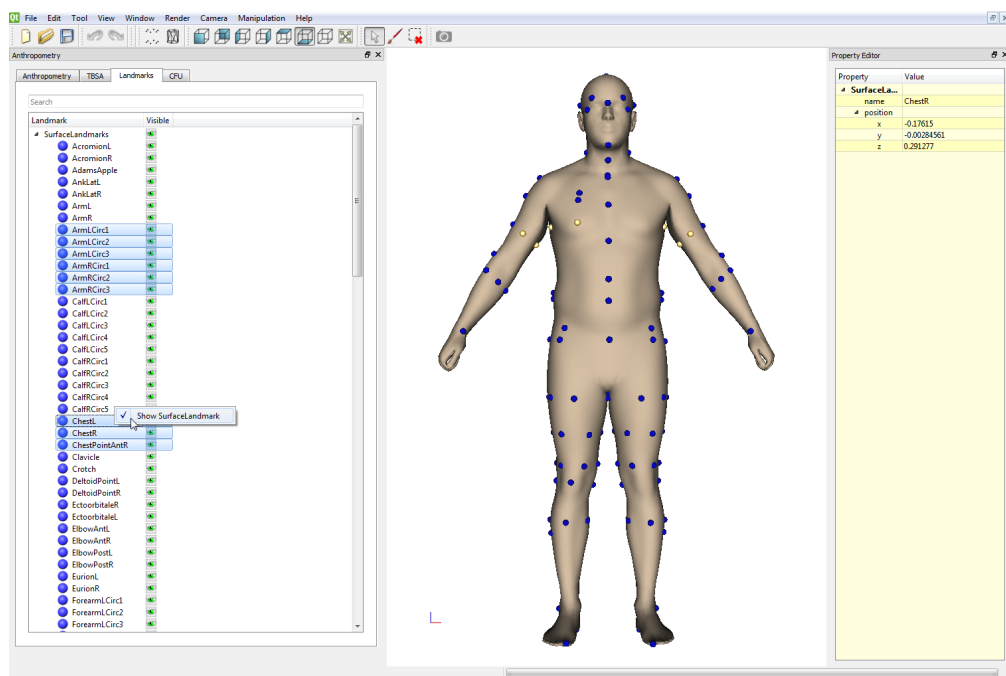


Figure 24. In the Landmarks tab, the display of body landmarks are controlled and visualized as blue spheres. Positional information of that point is displayed on the right panel and can be adjusted if necessary.

To better visualize the selected anthropometry features when the user clicks on “show” or “show only”, the model automatically become semi-transparent. Clicking on “hide” not only hides the selected features but also restores the full opacity to the model (Figure 25).

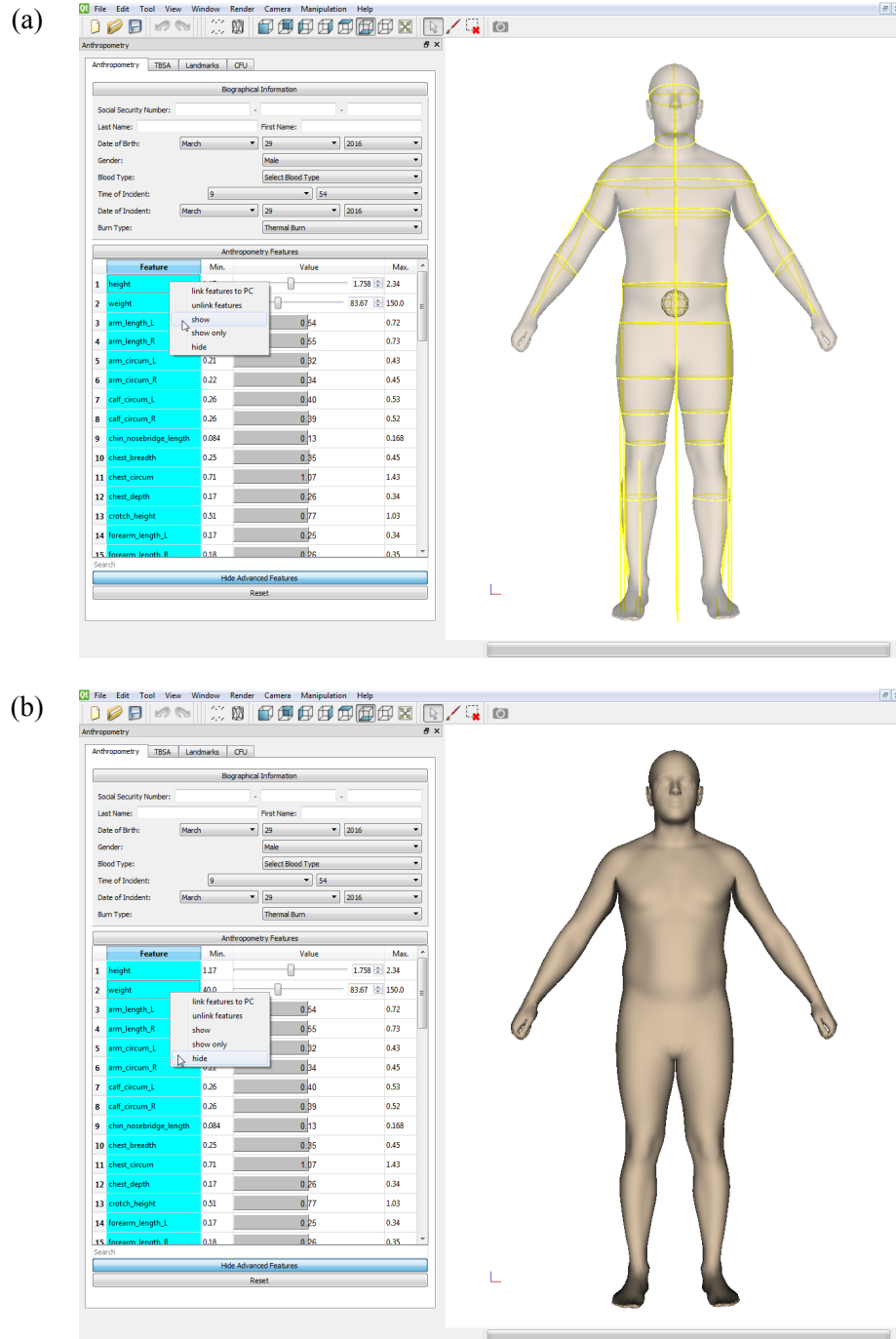
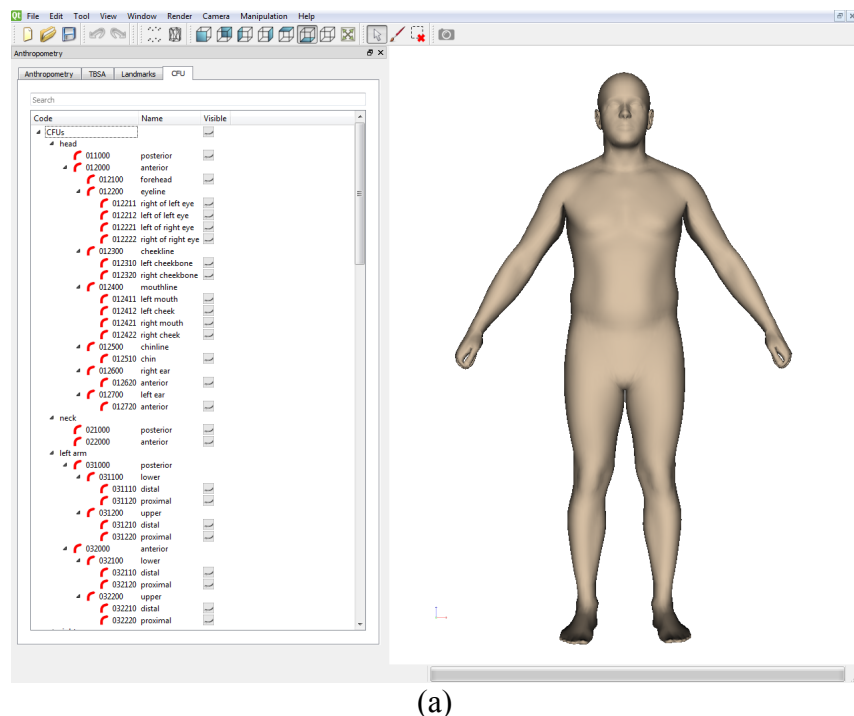


Figure 25: (a) The model automatically becomes semi-transparent when visualizing anthropometry features. (b) Hiding the features restores the full opacity of the model.

2.6.2. CFU

In the GUI, an additional tab for CFU, which is populated by the CFU definitions stored in a modifiable CSV file, was developed (Figure 26). In addition to grouping based on 25 major body parts (head, neck, left/right arm, left/right torso, left/right buttock, left/right leg, left/right foot, left/right front/back of hand, left/right crotch, and groin), it is also grouped into posterior/anterior and further sub-regions such as upper and lower, eyeline, cheekline, mouthline and chinline. Triangle indices from the mesh belonging to each CFU code are read in from the CSV file and are assigned a distinct color for visualization. Furthermore, the visualization of each CFU can be controlled by clicking on the visible icon individually. For groups of CFUs, multiple CFUs can be selected and right click to check the “Show CFU” box (Figure 27). Specifically for the hands where we have multiple CFU codes for the same surface, changing the visibility of any one CFU will alter the other CFUs which share the same triangles. For the typical end-user, this tab is not usually needed. However, it may be useful for advanced users who wish to develop their customized CFUs by redefining the triangle indices of the mesh to each CFU. The same functionality applies to both male and female body shapes.



(a)

(a)

Code	Name	Visible
CFUs		
head		
011000	posterior	
012000	anterior	
012100	forehead	
012200	eyeline	
012211	right of left eye	
012212	left of left eye	
012221	left of right eye	
012222	right of right eye	
012300	cheekline	
012310	left cheekbone	
012320	right cheekbone	
012400	mouthline	
012411	left mouth	
012412	left cheek	
012421	right mouth	
012422	right cheek	
012500	chinline	
012510	chin	
012600	right ear	
012620	anterior	
012700	left ear	
012720	anterior	
neck		
021000	posterior	
022000	anterior	
left arm		
031000	posterior	
031100	lower	
031110	distal	
031120	proximal	
031200	upper	
031210	distal	
031220	proximal	
032000	anterior	
032100	lower	
032110	distal	
032120	proximal	
032200	upper	
032210	distal	
032220	proximal	
right arm		

(b)

(c)

Code	Name	Visible
right arm		
041000	posterior	
041100	lower	
041110	distal	
041120	proximal	
041200	upper	
041210	distal	
041220	proximal	
042000	anterior	
042100	lower	
042110	distal	
042120	proximal	
042200	upper	
042210	distal	
042220	proximal	
left hand back		
051000	dorsal	
right hand back		
061000	dorsal	
left hand back		
071000	dorsal	
right hand back		
081000	dorsal	
left hand front		
092000	palmar	
right hand front		
102000	palmar	
left hand front		
112000	palmar	
right hand front		
122000	palmar	
left hand front		
132000	palmar	
right hand front		
142000	palmar	
left torso		
151000	posterior	
151100	lower	
151200	upper	
152000	anterior	
152100	lower	
152200	upper	
right torso		

(d)

Code	Name	Visible
right torso		
161000	posterior	
161100	lower	
161200	upper	
162000	anterior	
162100	lower	
162200	upper	
left buttock		
171000	posterior	
right buttock		
181000	posterior	
left leg		
191000	posterior	
191100	lower	
191110	distal	
191120	proximal	
191200	upper	
191210	distal	
191220	proximal	
192000	anterior	
192100	lower	
192110	distal	
192120	proximal	
192200	upper	
192210	distal	
192220	proximal	
right leg		
201000	posterior	
201100	lower	
201110	distal	
201120	proximal	
201200	upper	
201210	distal	
201220	proximal	
202000	anterior	
202100	lower	
202110	distal	
202120	proximal	
202200	upper	
202210	distal	
202220	proximal	
left foot		
211000	posterior	

(e)

Code	Name	Visible
left foot		
211000	posterior	
211100	lower	
211200	upper	
212000	anterior	
212100	lower	
212200	upper	
right foot		
221000	posterior	
221100	lower	
221200	upper	
222000	anterior	
222100	lower	
222200	upper	
left crotch		
231000	anterior	
right crotch		
241000	anterior	
groin		
251000	anterior	

Figure 26. (a) CFU tab in the GUI where CFU codes are grouped based on hierarchy in the CFU tab of the GUI. All 144 CFU codes are listed in descending order from b to e.

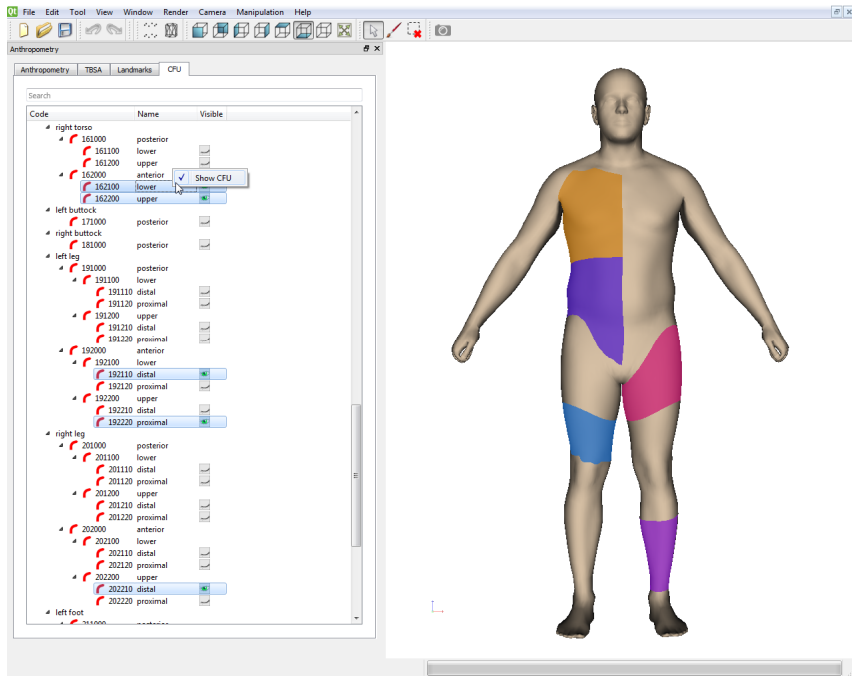


Figure 27. Visibility of each CFU can be controlled individually or in selected groups.

Additionally, the search algorithm to the CFUs was improved such that any keywords entered will display the entire tree of the CFU rather than just the hierarchical level containing those keywords (Figure 28).

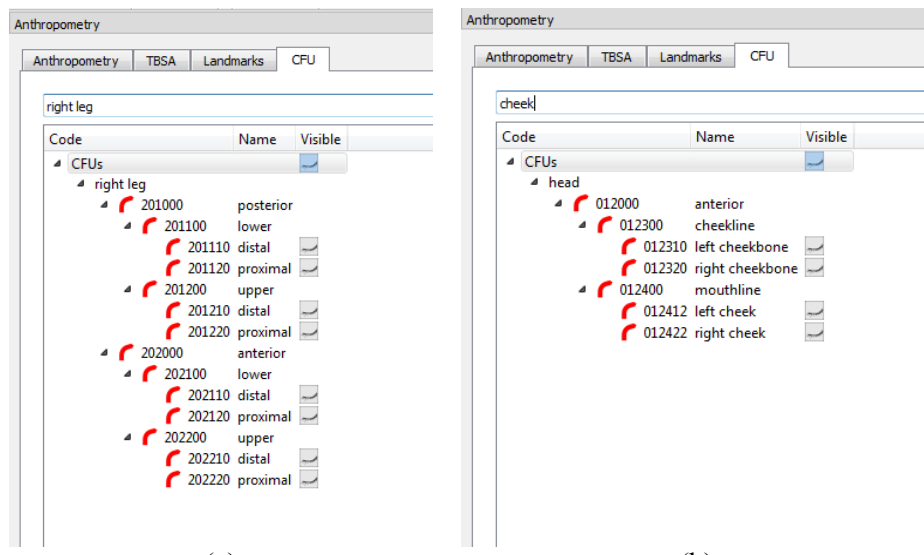
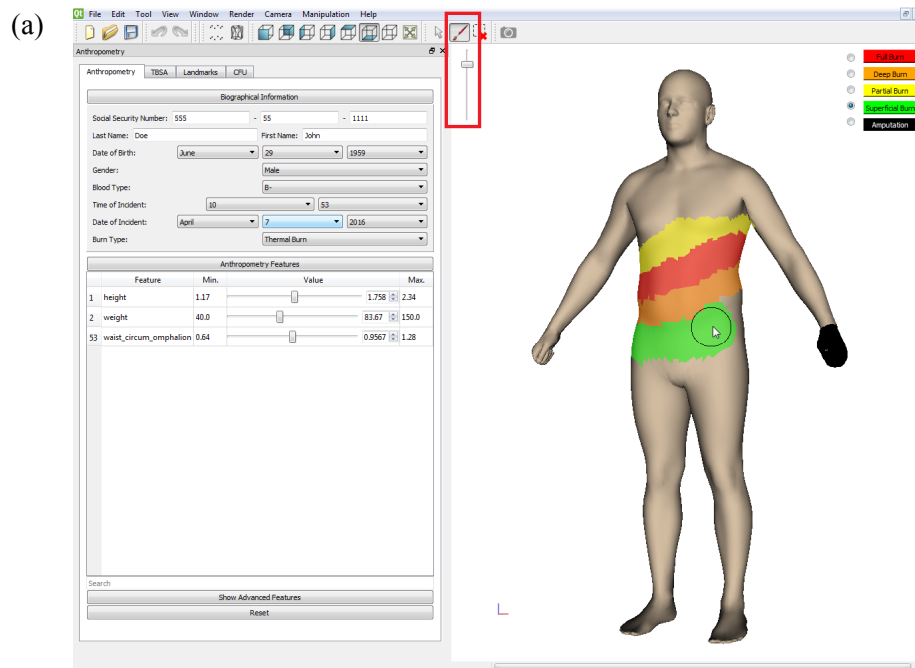


Figure 28: Examples of the improved keyword search of the CFUs. (a) Searching with main body segment keywords, such as right leg, and (b) lower hierarchical keywords, such as cheek, will result in the entire CFU displayed.

2.6.3. Demarcation Tools

A mesh surface demarcation capability was added to the GUI which includes painting of the mesh surface using a circle brush tool by selecting the paint brush icon on the top taskbar. For greater control of the burn area demarcation, an adjustable slider to control for size of circle brush in surface painting tool appears when the painting button is selected and disappears when other buttons are selected (icon boxed in red in Figure 29a). The radius of the circle can be increased or decreased by moving the slider up and down, respectively. Pressing the painting button also makes available radio buttons for the selection of different burn severity, full (red), deep (orange), partial (yellow) and superficial (green), as well as amputation (black). To paint, pressing the “Ctrl” key and left mouse button while moving the mouse over the region of interest highlights it interactively (Figure 29a). Highlighted regions can be erased by pressing the “Shift” key and selecting the area for elimination (Figure 29b). Once a surface triangle of the mesh has been demarcated a specific burn severity, it cannot be overridden. This ensures there is no accidental selection of an already defined area. Additionally, only demarcated areas of the selected burn severity can be erased by pressing the “Ctrl” key while moving the mouse over the region of interest, other highlighted burn severity areas will be unaffected. We will develop an override for this restriction in the potential Phase II by having the user deactivating this ability. The “Clear selection” button will clear all demarcations only for that demarcation selected (icon boxed in blue in Figure 29b). Furthermore, for better visualization and control of the 5 different demarcated surfaces, the visibility of each can be turned on and off by pressing their respective push buttons (Figure 29c).



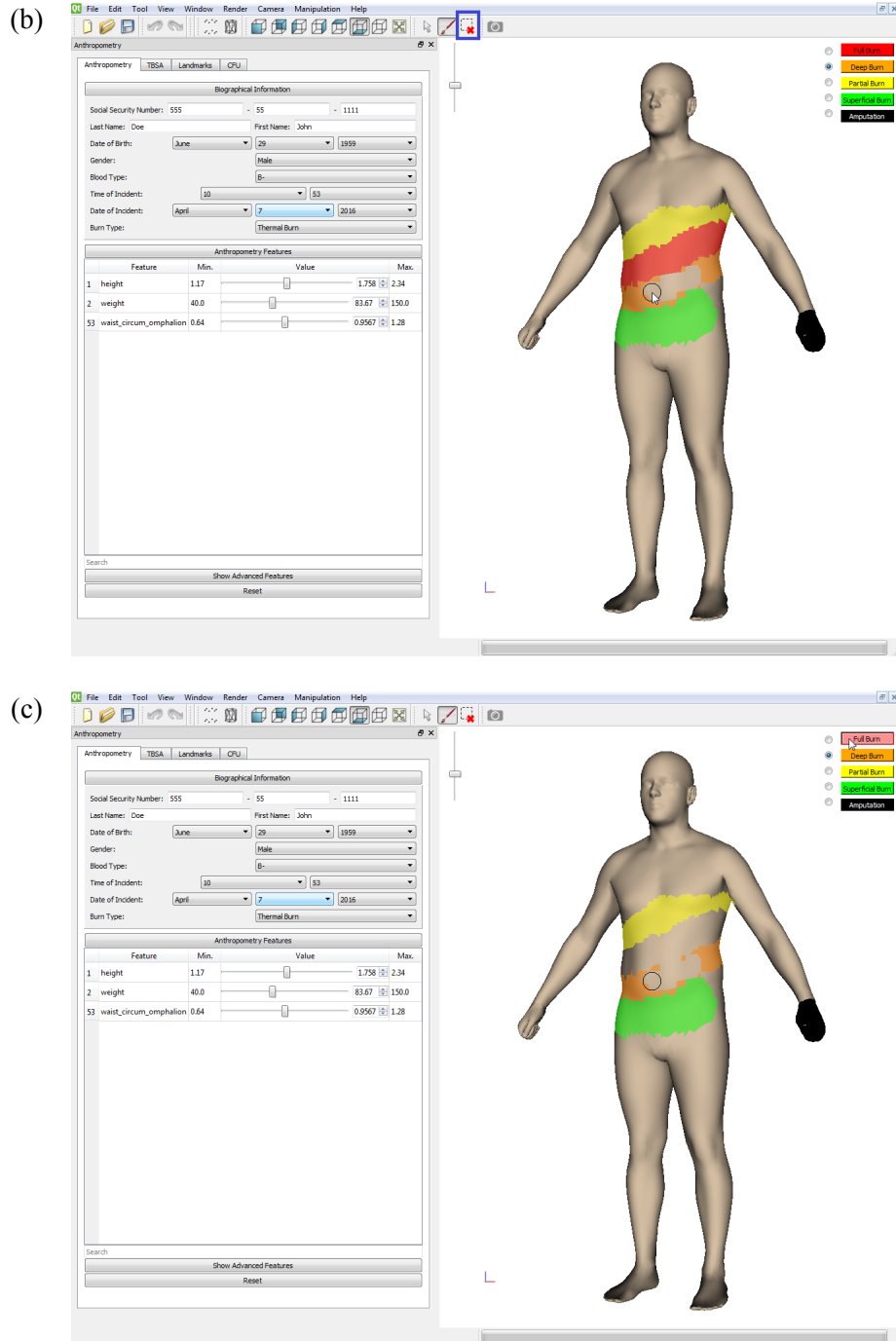


Figure 29. Screenshot of the GUI with the 4 different burn severity selections highlighted in different colors (full (red), deep (orange), partial (yellow) and superficial (green)) along with black for amputation. (a) When paint brush icon is pressed, an adjustable slider controlling the size of the circular painting brush appears (boxed in red). (b) Interactive erasing of highlighted demarcations. A clear selection icon is available for deleting all selections for specific demarcation (boxed in blue). (c) Visibility of all demarcations can be controlled by toggling the respective push buttons. In this example, demarcations for full burn are hidden, while the rest are made visible.

2.6.4. Burn Area Reporting

To present a concise reporting of the burn areas for each burn severity and each CFU, a TBSA tab was developed in the GUI. Upon initialization, the TBSA and all the CFUs are displayed in the lower portion in the tab awaiting entries for the 4 different burn severity plus amputation after demarcation. At the upper portion of the TBSA tab, the recommended fluids (Lactated Ringer's, colloid and D5W) according to different formulae will be displayed (Figure 30).

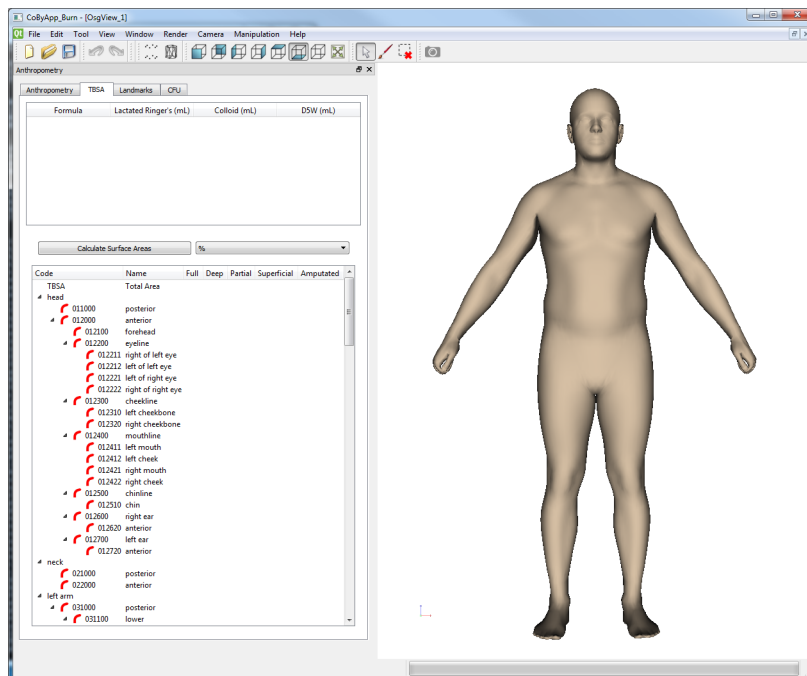


Figure 30. Screenshot of the TBSA tab in the burn assessment tool upon initialization.

After demarcation, the “Calculate Surface Areas” button in the middle of the tab is pressed to calculate and update the surface areas. Selection can be made to display percentage burn or absolute cm² values by changing the drop down menu right next to the calculate button (Figure 31). The top section of the tab lists fluid recommendations (Lactated Ringer's, Colloid, and D5W) according to the Brooke and Parkland formula (Figure 31). The Brooke formula recommends 1.5 mL of Lactated Ringer's solution per kg per %TBSA burn consisting of second (deep and partial) and third (full) degree, 0.5 mL of colloid per kg per %TBSA burn, and 2000 mL of D5W (dextrose 5% water) [24]. For the Parkland formula, 4 mL of Lactated Ringer's solution per kg per %TBSA burn is recommended instead [24]. Weight used is one of the anthropometry feature measurements entered by the user in the Anthropometry tab. Fluid recommends from other formulae can be included as well. In the lower tab, total burn surface areas for the 4 different burn severities plus amputation are listed as well as only the CFUs that have been demarcated. The non-demarcated CFUs have zero surface areas and are hidden. This will allow the user to quickly focus on the burn areas of the body. Furthermore, the entries to the 4 different burn severities are color coded accordingly for easy reading (Figure 31).

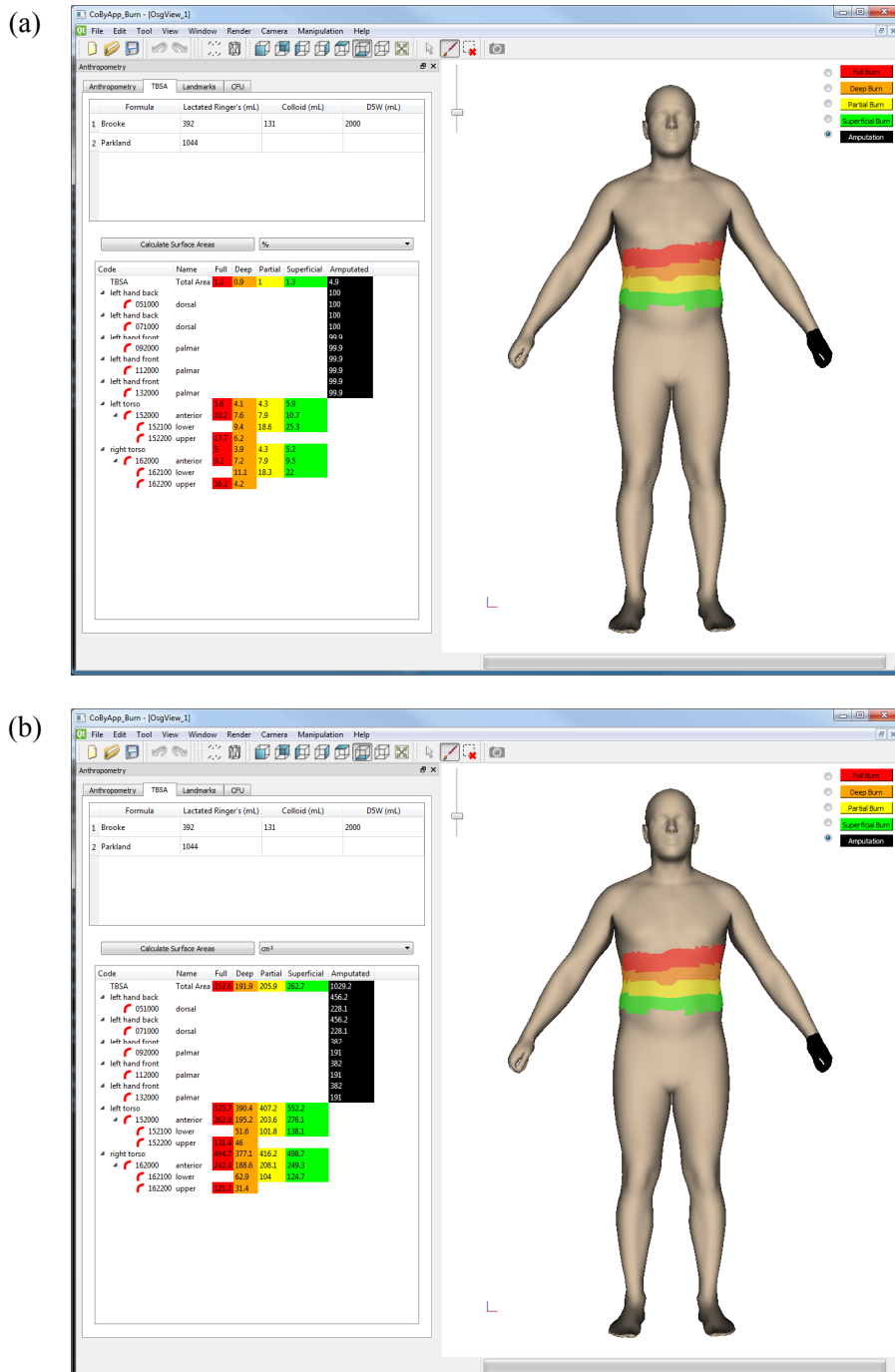
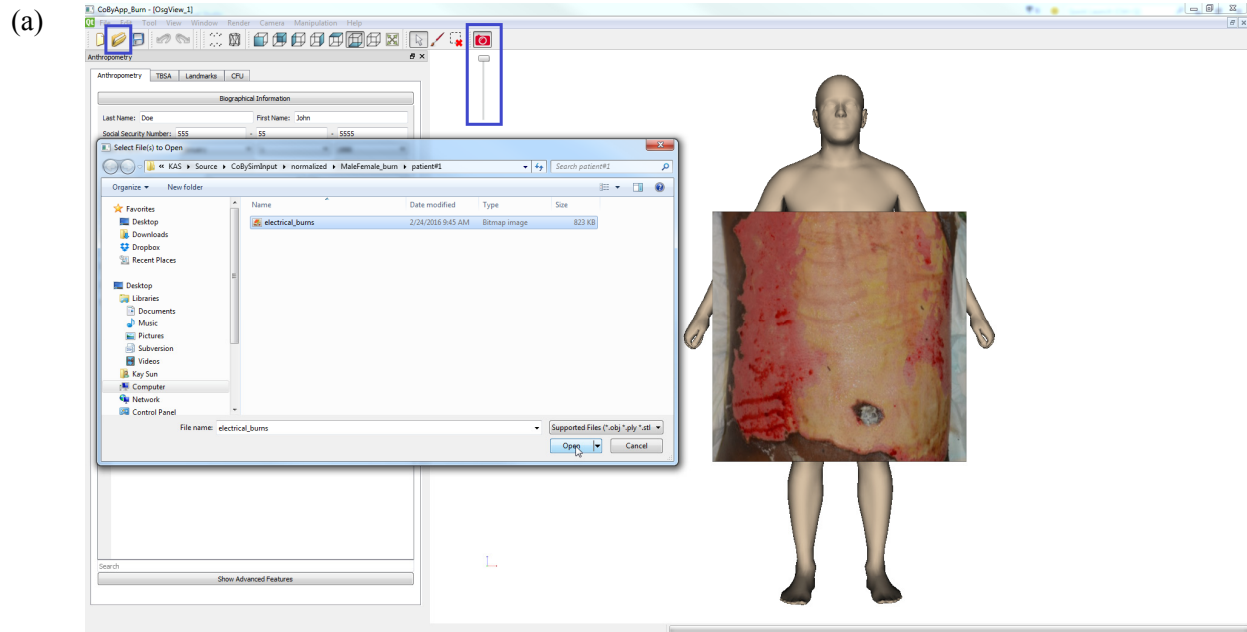


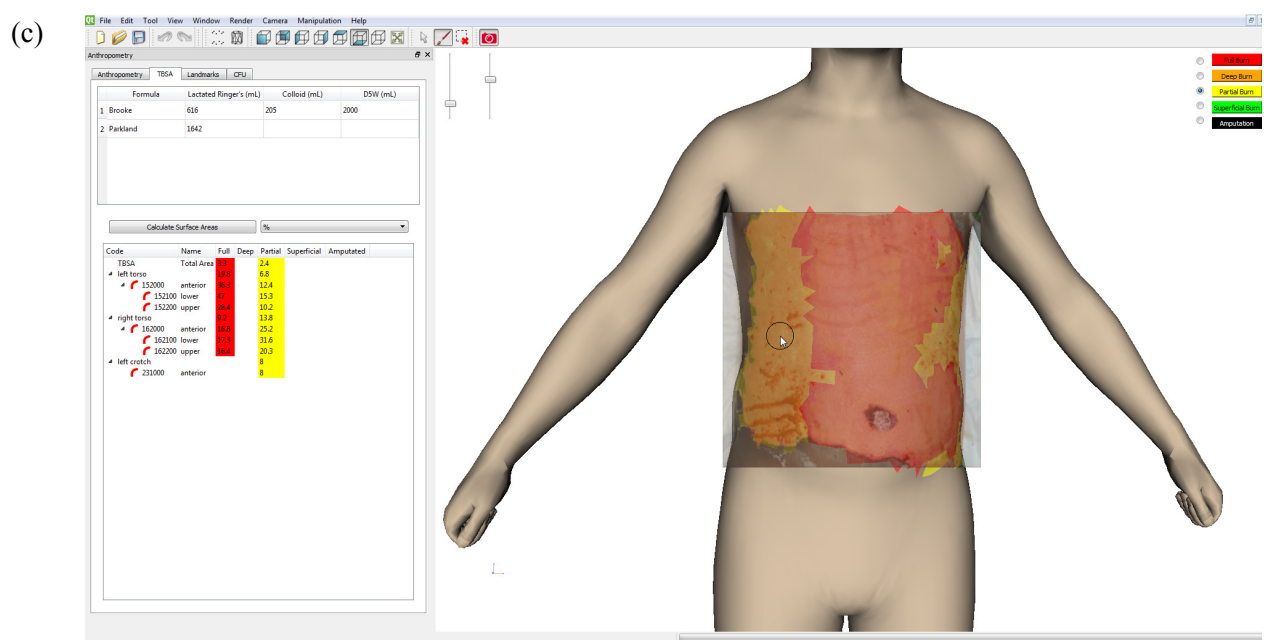
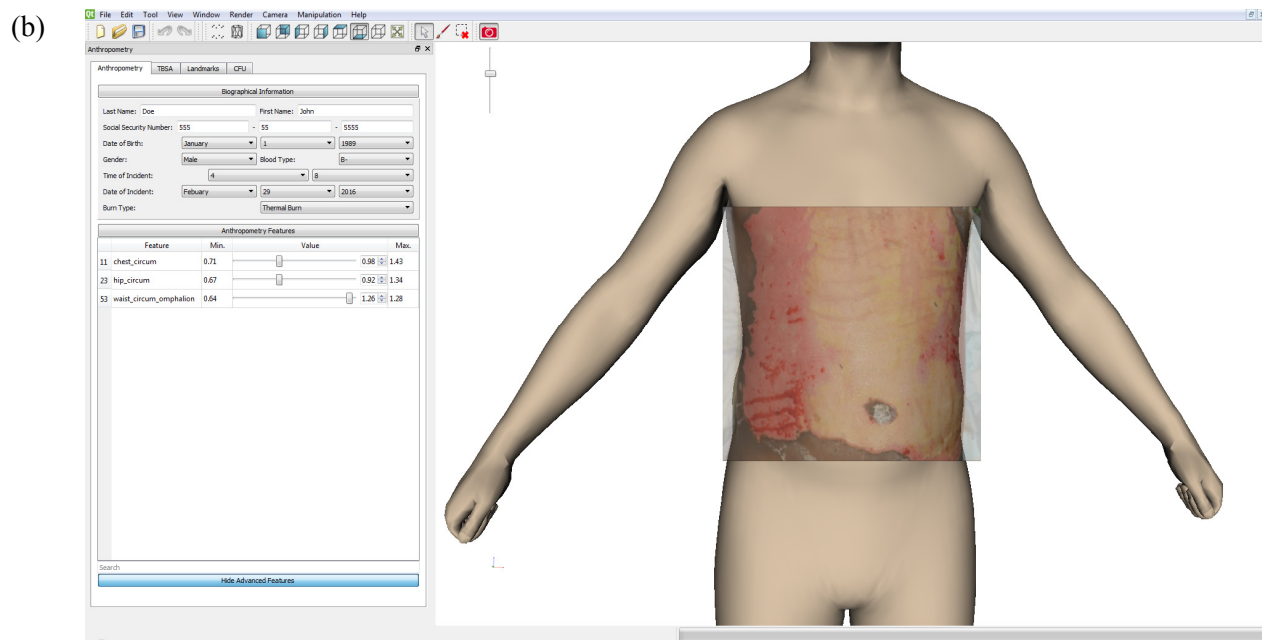
Figure 31. Screenshots of the TBSA report in (a) percentage and (b) absolute cm². At the bottom, total burn areas for each burn severity plus amputation are listed on the top along with just the CFUs that are demarcated. Both are color coded based on burn severity. At the top is the fluid recommendation according to Brooke and Parkland formulae.

2.6.5. Image Assist Demarcation

In addition to human body shapes variability, burn wounds are also often irregular in shape and have varied distributions. Typically, patients with small scattered burns are scored higher

%TBSA overestimation compared to patients with a single large burn area [25]. There is also physician subjectivity when they transcribe wounds from the actual patient onto 2D or 3D models [26]. Physicians generally tend to overestimate burn areas rather than underestimate them [27]. Even the most experienced burn physicians routinely overestimated %TBSA by 20%, while the less experienced ones overestimated by up to 49% [1]. To eliminate physician subjectivity and obtain accurate, repeatable burn area demarcations, photographic images of the wounds, often taken to the burn severity and location, are loaded into the GUI and superimposed onto the 3D human body model by manual orientation and scaling. Upon loading an image, the image button, initially grayed out, is toggled on and a slider automatically appears to allow the user to adjust the opacity of the photo for better visualization (Figure 32a and b). The 3D model is interactively manipulated to align and match the image with the model. Ideally, the patient's anthropometry measurements should be entered first to obtain a personalized 3D model for image alignment. However, since the burn image was downloaded from the internet [28], these body shape details are unavailable. Therefore, only the chest, hip and waist circumferences were adjusted to get a better match the body with burn image (Figure 32b). Once aligned, the burn areas are then traced onto the model objectively, using the photo as a guide for a truer and quicker one-to-one transcription (Figure 32c). The image can be shown or hidden by toggling on or off the image button. In Figure 32d, the burn surfaces areas and Brooke and Parkland fluid recommendations are calculated. As a potential future work to test the software tool onto the mobile platform (Android), we will take advantage of the build-in camera in the tablet to direct user to take images of the patient at the correct zoom and angle for direct alignment with the 3D model without need for any post-processing registration. Furthermore, infrared thermal imaging can also be acquired for image alignment and the temperature map used for automatic burn severity demarcation. Small infrared camera attachments for smartphones and tablets (FLIR ONE [29]) are readily available, making this capability highly feasible and beneficial for use in the hospital.





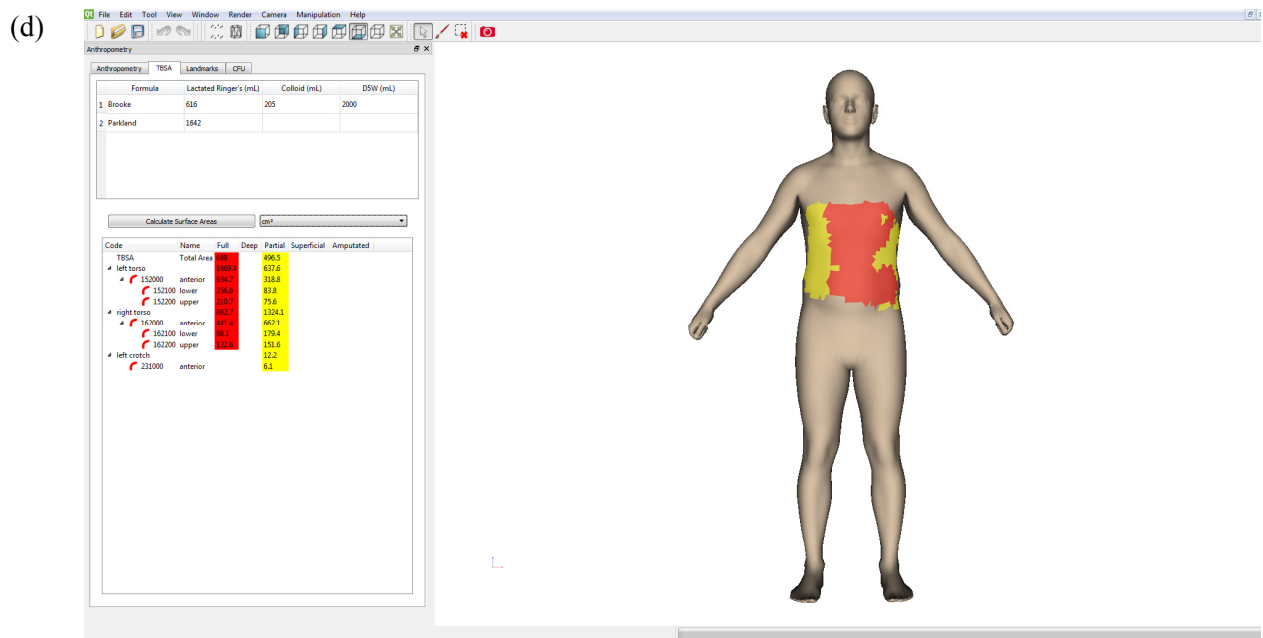


Figure 32. Screenshots of the image assisted demarcation. (a) The initial superpositioning of the loaded image (boxed in red) on top of the 3D model and the automatic appearance of the transparency control slider (boxed in blue). **(b)** Adjustment of the transparency slider changes the opacity of the loaded image for better visualization during manual alignment and tracing. **(c)** Tracing of the burn areas with different severity based on the image onto the 3D model and calculation of burn areas as percentage as well as fluid recommendations. **(d)** Calculated burn surface areas in cm^2 and fluid recommendations with image overlay turned off. The burn image shown was download from <http://burnssurgery.blogspot.com> [28].

2.7. Task 7: Project Management, Planning and Commercialization

Throughout the duration of the project, internal discussions and software reviews were carried out between members of the CFDRC team to ensure technical accuracy, satisfaction of software requirements and timely progression of project.

3. KEY RESEARCH ACCOMPLISHMENTS

In this Phase I project, we developed a functional prototype tool for real-time generation of an anthropometric 3D virtual human body with graphical annotations of burn areas and severity as well as assessment of %TBSA and fluid resuscitation recommendations.

We are pleased to report that the main goals of Phase I have been successfully accomplished and they include:

1. Generated in real-time virtual 3D human body model representation of the male and female burn patient using anthropometric inputs. The morphing of the 3D model is based on anthropometry data collected from ANSUR II survey.
2. Classified the mean male and female body surface according to our customized CFU definitions. Each CFU are colored differently and displayed in the GUI, along with the ability visualize each one individually or in groups. CFUs morphs with the deformed body surfaces.
3. Developed user tools for the visual annotation (add and erase) of demarcation areas based on burn severity as well as amputation with different highlighted colors. The size of the circle brush demarcation tool is controlled with an adjustable slider. Demarcations morphs with the deformed body surfaces.
4. Developed demarcated surface area reporting of the 4 different burn severities plus amputation based on the total body surface and each burned CFU. Non-burned CFUs are not displayed, while burned CFUs are color coded for the 4 different burn severities. Quick toggle between surface areas represented in percentage or absolute cm^2 . Fluid recommendations, based on Brooke and Parkland formulae, are calculated using %TBSA and displayed.
5. Developed the use of photographic images of burned body parts to assist in burn demarcations.

4. CONCLUSION

4.1 Project Importance and Implications

We have developed a burn injury assessment software tool that can generate in real-time, anthropometrically realistic virtual 3D human body model representation of the burn patient, which is subsequently used to demarcate burn areas based on burn severity and compute the %TBSA and fluid resuscitation recommendations. Photographic images of burned body parts can also be used to assist in burn demarcations. This tool may greatly improve the accuracy of TBSA and burn area estimations, and thereby %TBSA and ultimately treatment recommendations. Given physicians generally overestimate %TBSA with current traditional methods [27] with the most experienced burn physicians routinely overestimated %TBSA by 20%, while the less experienced ones overestimated by up to 49% [1], improvements in %TBSA and therefore proper burn treatments may ultimately result in better patient outcome and lower risk of complications.

In the U.S. alone, there are 127 specialized burn centers with another 4,500 acute care hospitals that will be just a download away from our software tool. The tool can also be used in telemedicine, whereby photographic images of burned body parts and patient's anthropometric measurements can be collected onto the tool and all that information can be securely shared with burn specialists at another location. Users can contact us on our website (www.medicalavatars.com) with regards to questions, comments, and bug reports. This will enable possible bugs and issues not detected during our internal testing to be identified and remedied.

4.2 Work Plans for Phase II

Successful proof-of-concept demonstrations in Phase I strongly justify the Phase I Option and Phase II continuation. For Phase I Option, the fully functional burn injury assessment prototype developed thus far for the desktop will be tested on a mobile platform, Android. Optimization of software and workflow will also be carried out to ensure ideal performance on the limited computing resources on the device. We will take advantage of the build-in camera in tablets to assist the user in taking the photo of the burned body part at the proper zoom and orientation by using the virtualized 3D patient model as a guide. Phase II effort will focus on the expansion, improvements and refinements of the functionalities developed in the prototype in Phase I as well as validation of the surface area calculations on burn patients. We plan to establish close collaboration with Prof. David Herndon from UTMB and Shriners Hospitals for Children, our consultant during Phase I, to test out our software tool on actual burn patients by physicians and nurses. The planned Phase II tasks are:

Analysis of children anthropometric data: Children anthropometric data from a published survey of 4000 subjects [30] will be divided into infant, child and youth for PCA and linear regression analyzes in order to obtain independent anthropometric controls for creating personalized children body model. 3D scans of children for morphing are available from a potential collaborator, Prof. Matthew P. Reed, from the University of Michigan Transportation Research Institute [31].

Body articulation: Full articulation of the joints in the ANSUR II models is needed to reach hard to reach body parts for burn demarcation, e.g armpits and groin regions. For an ongoing Army SBIR Phase II project, “WholeBody Anthropometric Design Models for Protective Equipment Design” with Alex Zhou as PI, a skeletal framework has been added to the ANSUR II male model, enabling full body articulation of not only the skin but also deformations of the complete internal organs, including muscle, blood vessels, nerves, bones, lungs, heart, liver, etc. The skeletal framework also scales with morphing along with all the internal organs. This skeletal framework will be added to the female model as well.

Burns to hands: Hands are one of the top body parts to get burned and the quality of life of burn survivors is determined greatly by how much dexterity is recovered in the hands [19]. However, the hands are in closed positions in the current ANSUR II models, making it difficult to accurately demarcate. An articulating framework as described previously for the whole body will be developed specifically for the hands, including each finger and joints. This will allow the hands to be opened up for CFU classification and mesh refinements if necessary. A dedicated GUI window will be developed to focus on the hands where hand breadth and length can be adjusted in real-time.

Real-time 3D head reconstruction: The complexities of the human face cannot be fully captured by facial anthropometric measurements alone. They can be readily captured on video by panning the camera around the head and perform real-time 3D head reconstruction. This creates a 3D surface of the face and head plus texture information for burn demarcation right on the model itself. The reconstructed head and morphed body surfaces can then be stitched together. The Robotics Institute at Carnegie Mellon University, a collaborator on an upcoming SBIR Phase I project - “Protective Mask Sizing App” with Kay Sun as the PI, has developed this technology [32] and will be working with us to customize it towards predicting protective mask sizes. Similarly, this application can be extended for personalized facial burn demarcations.

Patient database: Patient data entered (name, gender, age, anthropometric measurements), collected (photographic images), and all generated and processed data (3D body shape model, burn surfaces, %TBSA, %CFU) will be organized and stored in an open-source database management system (MS-SQL or Oracle). This type of relational file management system is highly flexible, scalable to a large number of patients and adaptable to additional file formats as well as potentially translatable to web applications for telemedicine. The database will be designed for easy navigation organized by each patient for different data types and dates. Additionally, multiuser can interact at any point of the workflow using synced data from the database. One user can stop the workflow midway, saving all entered data into the database, and another user can subsequently continue with the workflow by reloading all the data from the database.

Noninvasive burn depth determination: Infrared thermal imaging can be used to measure differences in temperature between burned and healthy skin, which are then related to burn depth [33]. Thermal images can now be captured on mobile devices with the latest FLIR One (FLIR Systems, Inc). It is an infrared camera attachment for the iPhone (snaps onto back) and Android phones/tablet (via mini-USB). This solution preserves the portability aspect of our tool and

expands its potential functionality to automatically determine burn depth, thereby eliminating the need to manually demarcate different burn severity areas. Our collaborator on a previous effort, Prof. Ioannis Pavlidis from the University of Houston, is an expert in measurements of human physiology using thermal imaging, who can help develop this highly beneficial capability with us.

Validation of surface area calculations on burn patients: Validation of the %TBSA and %CFU calculated will be performed on burn patients with the assistance of our collaborator, Prof. Herndon, who has access to burn centers, UTMB and Shriners Hospitals for Children in Galveston. In addition to Prof. Herndon, Drs. Ludwik K. Branski, Paul Wurzer and Gabriel Hudshagen, and Deb Benjamin from both hospitals have all agreed to participate in using our software tool for validation and offer feedback. We will work with the university, hospital and Prof. Herndon for the proper approvals and patient consent to conduct this study.

Additionally, we can satisfy all the environment and platform requirements requested. The software prototype is required to run on virtual machines in the Development/Validation Environment (DVE) of the U.S. Army that uses Windows 2008R2 server, MS-SQL or Oracle database and Windows 7 operating systems. The desktop version of our software prototype was and will continue to be developed on Windows 7. We also have Windows server and VMware on hand to test out the virtual desktop functionalities together with the patient database (MS-SQL or Oracle) we planned to develop. We will work with the Army to transfer our software prototype onto their specific U.S. Army Medical Command (MEDCOM) environment and accommodate any changes required.

5. PUBLICATIONS, ABSTRACTS, AND PRESENTATIONS

An abstract listed below was submitted to the 2016 Military Health System Research Symposium (MHSRS) under the Burn & Intensive Care session topic. The full abstract is in Section 10.

Burn Injury Assessment Tool with Morphable 3D Human Body Models

Kay Sun, PhD¹, Michael Rossi, MS¹, Xianlian (Alex) Zhou, PhD¹, Vincent Harrand, PhD¹, Andrzej Przekwas, PhD¹, David Herndon, MD^{2,3}

¹CFD Research Corporation, Huntsville, AL.; ²University of Texas Medical Branch, Galveston, TX.; ³Shriners Hospitals for Children, Galveston, TX.

6. INVENTIONS, PATENTS AND LICENSES

Nothing to report.

REPORT OF INVENTIONS AND SUBCONTRACTS		<i>(Pursuant to "Patent Rights" Contract Clause. See Instructions on Reverse Side)</i>	
<p><i>Form Approved OMB No. 9000-0095 Expires Aug 31, 2001</i></p> <p>The public reporting burden for this collection of information is estimated to average 1 hour per response, including the time for reviewing instructions, searching existing data sources, gathering and maintaining the data needed, and completing and reviewing the collection of information. Send comments regarding this burden estimate or any other aspect of this collection of information, including suggestions for reducing the burden, to Department of Defense, Directorate for Information Operations and Reports (9000-0095), 1215 Jefferson Davis Highway, Suite 1204, Arlington, VA 22202-4322. Respondents should be aware that notwithstanding any other provision of law, no person shall be subject to any penalty for failing to comply with a collection of information if it does not display a currently valid OMB control number.</p> <p>PLEASE DO NOT RETURN YOUR COMPLETED FORM TO THIS ADDRESS. RETURN COMPLETED FORM TO THE CONTRACTING OFFICER.</p>			
1a. NAME OF CONTRACTOR/SUBCONTRACTOR	c. CO-CONTACT NUMBER	2a. NAME OF GOVERNMENT/PATENT CONTRACTOR	c. CO-CONTACT NUMBER
d. ADDRESS <i>Freelance ZIP Code:</i>	d. ADDRESS DATE <i>15/09/24</i>	d. AWARDED DATE <i>15/09/24</i>	w/81XXWH-15-C-0148
b. ADDRESS <i>Freelance ZIP Code:</i>	b. ADDRESS <i>701 McMillian Way NW, Suite D Huntsville, AL 35806</i>	b. FROM	15/09/24
b. TO		b. TO	16/04/23
SECTION I - SUBJECT INVENTION S			
5. "SUBJECT INVENTIONS" REQUIRED TO BE REPORTED BY CONTRACTOR/SUBCONTRACTOR (If "None" so state)		ELECTION TO FILE PATENT APPLICATION d. CONFIRMATORY INSTRUMENT OR ASSIGNMENT TO OWNER TO CONTRACTING OFFICER e. <input type="checkbox"/> YES <input checked="" type="checkbox"/> NO	
a. NAME OF INVENTOR (Last, First, M.I.) b.		b. TITLE OF INVENTION c.	
c. NAME OF INVENTOR (Last, First, M.I.) d.		d. TITLE OF INVENTION e.	
f. EMPLOYER OF INVENTOR (Not Employee by Contract) <input checked="" type="checkbox"/> (1a) NAME OF INVENTOR (Last, First, M.I.) (2a) NAME OF INVENTOR (Last, First, M.I.)		g. ELECTED TO FILE IN COUNTRY <input checked="" type="checkbox"/> UNITED STATES <input type="checkbox"/> OTHER (1) TITLE OF INVENTION (2) FOR REIN CO-UNRIES OF PATENT APPLICATION	
d. NAME OF EMPLOYER (1) ADDRESS OF EMPLOYER (Last, First, M.I.)		f. SUBCONTRACTOR g. SUBCONTRACT NUMBER h. SUBCONTRACT DATE	
SECTION II - SUBCONTRACTS (Containing a "Patent's Rights" Clause)			
6. SUBCONTRACTS AWARDED BY CONTRACTOR/SUBCONTRACTOR (If "None" so state)		i. SUBCONTRACT NUMBER j. DATE k. NUMBER	
m. NAME OF SUBCONTRACTOR n. ADDRESS (Last, First, M.I.)		o. DESCRIPTION OF WORK TO BE PERFORMED UNDER SUBCONTRACT p. ESTIMATED COMPLETION	
SECTION III - CERTIFICATION			
q. CERTIFICATION OF REPORT BY CONTRACTOR/SUBCONTRACTOR (Not required if "Patent Rights Clause") I certify that the reporting party has procedures for prompt identification and timely disclosure of "Subject Inventions," that such procedures have been followed and that all "Subject Inventions" have been reported.			
a. Name of Authorized Contractor/Subcontractor Official (Last, First, Middle Initial) Deborah A. Phipps		b. TITLE Contracts Manager 	
		c. SIGNATURE 	
		d. DATE SIGNED 04/22/16	
PREVIOUS EDITION MAY BE USED.			

7. REPORTABLE OUTCOMES

In this Phase I project, we have developed a functional burn injury assessment software prototype that can generate in real-time, anthropometrically realistic virtual 3D human body model representation of the burn patient, which is subsequently used to demarcate burn areas based on burn severity and compute the %TBSA and fluid resuscitation recommendations. Photographic images of burned body parts can also be used to assist in burn demarcations (Figure 33). A live demonstration of our software tool was performed for personnel from U.S. Army Institute of Surgical Research (USAISR) on March 2nd 2016.



Figure 33. Our burn injury assessment software prototype, CoBi_Burn.



Figure 34. Cover slide to the project update and software demonstration meeting with USAIRS.

8. OTHER ACHIEVEMENTS

Nothing to report.

9. REFERENCES

- [1] L. S. Nicther, C. A. Bryant, and R. F. Edlich, "Efficacy of burned surface area estimates calculated from charts--the need for a computer-based model.," *J. Trauma*, vol. 25, pp. 477–481, 1985.
- [2] R. Richard, J. A. Jones, and P. Parshley, "Hierarchical Decomposition of Burn Body Diagram Based on Cutaneous Functional Units and Its Utility," *J. Burn Care Res.*, vol. 36, pp. 33–43, 2015.
- [3] S. Hettiaratchy and R. Papini, "Initial management of a major burn: I--overview.," *BMJ*, vol. 328, no. 7455, pp. 1555–1557, 2004.
- [4] M. B. B. Klein, "Thermal, chemical, and electrical injuries.,," in *Grabb and Smith's Plastic Surgery*, 7th editio., C. H. Thorne, Ed. LWW, 2007, pp. 132–148.
- [5] S. Hettiaratchy and R. Papini, "Initial management of a major burn: II—assessment and resuscitation," *BMJ*, vol. 329, pp. 101–103, 2004.
- [6] N. D. Rossiter, P. Chapman, and I. A. Haywood, "How big is a hand?," *Burns*, vol. 22, pp. 230–231, 1996.
- [7] G. A. Knaysi, G. F. Crikelair, and B. Cosman, "The Rule of Nines: Its history and accuracy," *Plast. Reconstr. Surg.*, vol. 41, no. 6, pp. 560–563, 1968.
- [8] C. C. Lund and N. C. Browder, "The estimation of areas of burns," *Surgery, Gynaecol. Obstet.*, vol. 79, pp. 352–358, 1944.
- [9] T. L. Wachtel, C. C. Berry, E. E. Wachtel, and H. A. Frank, "The inter-rater reliability of estimating the size of burns from various burn area chart drawings," *Burns*, vol. 26, pp. 156–170, 2000.
- [10] E. H. Livingston and S. Lee, "Percentage of burned body surface area determination in obese and nonobese patients.," *J. Surg. Res.*, vol. 91, pp. 106–110, 2000.
- [11] D. G. Greenhalgh, "Burn resuscitation," *J Burn Care Res*, vol. 28, no. 4, pp. 555–565, 2007.
- [12] B. Allen, "Learning body shape models from real-world data," *Ph.D. Thesis, Dep. Comput. Sci. Eng. Univ. Washingt.*, 2005.
- [13] C. C. Gordon, T. Churchill, C. E. Clauser, J. T. Mcconville, I. Tebbetts, and R. a Walker, "2012 Anthropometric Survey of U . S . Army Personnel : Methods and Summary Statistics," 2014.
- [14] V. Blanz and T. Vetter, "A morphable model for the synthesis of 3D faces," *Proc. 26th Annu. Conf. Comput. Graph. Interact. Tech. - SIGGRAPH '99*, pp. 187–194, 1999.
- [15] S. Paquette, C. Gordon, and B. Bradtmiller, "Anthropometric Survey (ANSUR) II Pilot Study: Methods and Summary Statistics,Technical Report, NATICK/TR-09/014," 2009.
- [16] J. Hotzman, C. Gordon, B. Bradtmiller, B. D. Corner, M. Mucher, S. Kristensen, and C. L. Blackwell, "Measurer's handbook : US Army and Marine Corps anthropometric surveys 2010-2011," *Tech. Rep. NATICK/TR-11/017*, no. September 2009, pp. 2010–2011, 2011.
- [17] R. L. Richard, M. E. Lester, S. F. Miller, J. K. Bailey, T. L. Hedman, W. S. Dewey, M. Greer, E. M. Renz, S. E. Wolf, and L. H. Blackbourne, "Identification of Cutaneous Functional Units Related to Burn Scar Contracture Development," *J. Burn Care Res.*, vol. 30, no. 4, pp. 625–631, 2009.
- [18] R. L. Richard, W. S. Dewey, W. R. Anyan III, J. Kemp-Offenberg, D. Murray, M. Shetler, D. P. Hawkins, J. A. Jones, and I. H. Faraklas, "Cutaneous Functional Unit is a better index than Total Body Surface Area related to burn patient outcomes," *J. Burn Care Res.*,

vol. 35, no. 3, p. S77, 2014.

- [19] S. R. Sabapathy, B. Bajantri, and R. R. Bharathi, "Management of post burn hand deformities," *Indian J. Plast. Surg.*, vol. 43, no. Suppl, pp. S72–S79, 2010.
- [20] R. D. Mosteller, "Simplified calculation of body-surface area.," *N. Engl. J. Med.*, vol. 317, no. 17, p. 1098, 1987.
- [21] D. Du Bois and E. F. Du Bois, "A formula to estimate the approximate surface area if height and weight be known. 1916.," *Nutrition*, vol. 5, no. 5, pp. 303–311, 1989.
- [22] G. B. Haycock, G. J. Schwartz, and D. H. Wisotsky, "Geometric method for measuring body surface area: A height-weight formula validated in infants, children, and adults," *J. Pediatr.*, vol. 93, no. 1, pp. 62–66, 1978.
- [23] E. A. Gehan and S. L. George, "Estimation of human body surface area from height and weight.," *Cancer Chemother. Rep.*, vol. 54, no. 4, pp. 225–35, 1970.
- [24] S. L. Hansen, "From cholera to 'fluid creep': a historical review of fluid resuscitation of the burn trauma patient.," *Wounds*, vol. 20, no. 7, pp. 206–13, 2008.
- [25] D. Parvizi, L. P. Kamolz, M. Giretzlehner, H. L. Haller, M. Trop, H. Selig, P. Nagele, and D. B. Lumenta, "The potential impact of wrong TBSA estimations on fluid resuscitation in patients suffering from burns: Things to keep in mind," *Burns*, vol. 40, no. 2, pp. 241–245, 2014.
- [26] J. M. Neuwalder, C. Sampson, K. H. Breuing, and D. P. Orgill, "A review of computer-aided body surface area determination: SAGE II and EPRI's 3D Burn Vision.," *J. Burn Care Res.*, vol. 23, no. 1, pp. 55–59, 2002.
- [27] L. P. Kamolz, D. Parvizi, M. Giretzlehner, and D. B. Lumenta, "Burn surface area calculation: What do we need in future," *Burns*, vol. 40, no. 1, pp. 171–172, 2014.
- [28] "<http://burnssurgery.blogspot.com/2012/07/electrical-flash-burns-outcome.html>." .
- [29] "FLIR ONE." [Online]. Available: <http://www.flir.com/flirone/content/?id=62910>.
- [30] R. G. Snyder, L. W. Schneider, C. L. Owings, H. M. Reynolds, H. Golomb, and A. Schork, "Anthropometry of Infants, Children and Youth To Age 18 For Product Safety Design," *Highw. Saf. Res. Institute, Univ. Michigan*, vol. UM-HSRI-77, 1977.
- [31] M. P. Reed, "UMTRI/CPS/C Child Anthropometry Study." [Online]. Available: http://mreed.umtri.umich.edu/mreed/downloads.html#child_anthro.
- [32] L. A. Jeni, J. F. Cohn, and T. Kanade, "Dense 3D Face Alignment from 2D Video for Real-Time Use," *Elsevier Image Vis. Comput.*
- [33] J. D. Medina-Preciado, "Noninvasive determination of burn depth in children by digital infrared thermal imaging," *Journal of Biomedical Optics*, vol. 18. p. 061204, 2012.

10. APPENDICES

Abstract to 2016 MHSRS

Burn Injury Assessment Tool with Morphable 3D Human Body Models

Kay Sun, PhD¹, Michael Rossi, MS¹, Xianlian (Alex) Zhou, PhD¹, Vincent Harrand, PhD¹, Andrzej Przekwas, PhD¹, David Herndon, MD^{2,3}

¹CFD Research Corporation, Huntsville, AL.; ²University of Texas Medical Branch, Galveston, TX.; ³Shriners Hospitals for Children, Galveston, TX.

Background

Burn patient outcomes are dependent on the surface area of the wound as percentage of total burn surface area (%TBSA), burn location(s), burn depth(s) and patient age. %TBSA is essential in determining burn treatment and rehabilitation. Conventional methods (Rule-of-Palm/Nines, Lund-Browder) may result in inaccurate %TBSA since a generic 2D body shape diagram representing the human body is used. This fixed 2D template fails to capture the 3D anthropometric variability of actual human body shapes. The objective of this project is to develop a burn injury assessment software tool that can create anthropometrically realistic 3D virtual human body models in real-time using anthropometry inputs. The 3D model is used to interactively demarcate burn areas based on severity and compute %TBSA to improve burn area estimations.

Method

Principal component analysis of the 3D male and female body scans collected from the latest Army anthropometry survey (ANSUR II¹) produces mean surface model, principal shapes and other data for each gender. The body generator uses this dataset to create realistic virtual model in real-time based on anthropometric measurements (height, weight, waist circumference, etc.). These measurements (52 for male; 51 for female) are automatically extracted from the 3D model by using typical geometric measurements, like length of straight line or polyline and planar intersection contours on the model surface, to connect their associated specific virtual landmarks positioned on the model. To facilitate the use of cutaneous functional units (CFU) in burn prognosis, which is a better indicator of burn scar contracture than %TBSA, the mean gender models were classified into CFUs ². The tool runs on Windows platform.

Results

With the tool, the user can enter the patient's biographical information (name, age, gender, burn type, etc.). Switching gender automatically loads the appropriate model. The user enters any anthropometry measurements available to create the personalized 3D model in real-time, which is displayed and can be manipulated (rotate, translate and zoom). The user can manually demarcate (add, erase) the 4 burn severities (full, deep, partial, superficial) plus amputation, distinguished by color, using a size adjustable painting tool, as well as control their visibility. A report with the absolute and relative burn surface area to the total body area and to each CFU for each burn severity is calculated and displayed. Photographic images of burned body parts can also be superpositioned onto the 3D model to trace the wounds to aid in the demarcation.

Conclusion

A software tool was developed that can generate in real-time, anthropometrically realistic virtual 3D body model representation of the patient, allow the user to demarcate burn areas of varying severity on the 3D model for calculation of burn areas, and use photographic images of burned body parts to assist in burn demarcations. This tool may improve the accuracy of TBSA and burn area estimations, and thereby %TBSA and ultimately treatment recommendations for the best patient outcome with minimal risk of complications.

References

1. Hotzman, J. et al. Tech. Rep. Natick/TR-11/017 2011.
2. Richard, R. et al. J. Burn Care Res. 2015.

Learning Objectives

1. Developed an interactive anthropometry-based human body generator to create, in real-time, a personalized 3D body shape model that has been morphed according to available anthropometric measurements (e.g. weight, age, gender, height, waist, arms and legs measurements).
2. Created a software Graphical User Interface (GUI) to display and manipulate (zoom, translate, rotate) personalized human body models, along with a demarcation capability in GUI to highlight areas on the 3D model surface for various burn severity and deletion for amputees.
3. Software calculates and reports the %TBSA and %CFU based on the demarcated burn surface area and human body surface area (TBSA or CFU) which varies with body shape and degree of amputation.



QUAD CHART

Burn Injury Assessment Tool with Morphable 3D Human Body Models



PI: Kay Sun | Organization: CFD Research Corporation | SBIR A151-055 Phase I | Award Amount: \$99,978.57

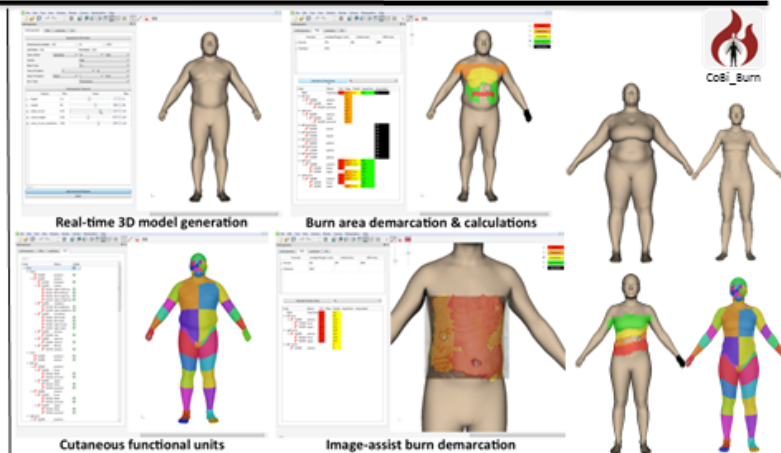
Study Goal

Develop a burn injury assessment tool with morphable 3D anthropometric human body models to improve the accuracy of percentage burn surface area (%TBSA) estimates.

Approach

Develop a burn injury assessment tool that can

- Generate in real-time virtual 3D anthropometric male/female body model.
- Interactive demarcation of burn areas with different severity and amputation.
- Calculate and report burns based on TBSA and cutaneous functional units (CFU) as well as fluid recommendations.
- Use photographic images of burned body parts to assist in burn demarcations.



Accomplishment: Developed a fully functional burn injury assessment tool.

Timeline and Cost

Activities	2015	2016	2017	2018
Prototype on Windows 7 (Phase I)				
Prototype on Android (Phase I Option)				
Patient Database (Phase II)				
Body Articulation (Phase II)				
Burns to Hands (Phase II)				
Burn Depth Estimation (Phase II)				
Patient Validation at UTMB (Phase II)				
Software Delivery (Phase II)				
Estimated Budget (\$)	50K	50K+50K	500K	500K

Updated: April 21 2016

Goals/Milestones

Phase I (2015 – 2016) – Prototype on Windows 7

Completed development of functional prototype on Windows 7.

Phase I Option (2016) – Prototype on Android

Testing of prototype on Android mobile platform.

Phase II (2017) – Expand capabilities

Patient database with printable outputs.

Full body and finger articulations.

Phase II (2018) – Expand capabilities and validation

Burns to hands.

Capture & integration of infrared images for burn demarcations.

Validation on burn patients at U. of Texas Medical Branch & Shriners Hospital for Children (Prof. David Herndon).

Budget Expenditure to Date

Projected: \$99,978.57

Actual : \$99,978.57